Developmental regulation of myeloerythroid progenitor function by the *Lin28b–let-7–Hmga2* axis

R. Grant Rowe,[1]* Leo D. Wang,[1,2,4]* Silvia Coma,[1] Areum Han,[1,5] Ronald Mathieu,[2,3] Daniel S. Pearson,[1] Samantha Ross,[1] Patricia Sousa,[1] Phi T. Nguyen,[2,4] Antony Rodriguez,[6] Amy J. Wagers,[2,4,8] and George Q. Daley[1,2,5,7,9,10]

[1]Stem Cell Transplantation Program, Stem Cell Program, Division of Pediatric Hematology/Oncology, Boston Children's Hospital and Dana-Farber Cancer Institute, Boston, MA 02215
[2]Harvard Stem Cell Institute, Cambridge, MA 02138
[3]Flow Cytometry Laboratory, Boston Children's Hospital, Boston, MA 02115
[4]Joslin Diabetes Center, Boston, MA 02215
[5]Department of Biological Chemistry and Molecular Pharmacology, Harvard Medical School, Boston, MA 02115
[6]Department of Molecular and Human Genetics, Baylor College of Medicine, Houston, TX 77030
[7]Howard Hughes Medical Institute, Boston, MA 02115
[8]Department of Stem Cell and Regenerative Biology, Harvard University, Cambridge, MA 02138
[9]Division of Hematology, Brigham and Women's Hospital, Boston, MA 02115
[10]Manton Center for Orphan Disease Research, Boston, MA 02115

For appropriate development, tissue and organ system morphogenesis and maturation must occur in synchrony with the overall developmental requirements of the host. Mistiming of such developmental events often results in disease. The hematopoietic system matures from the fetal state, characterized by robust erythrocytic output that supports prenatal growth in the hypoxic intrauterine environment, to the postnatal state wherein granulocytes predominate to provide innate immunity. Regulation of the developmental timing of these myeloerythroid states is not well understood. In this study, we find that expression of the heterochronic factor *Lin28b* decreases in common myeloid progenitors during hematopoietic maturation to adulthood in mice. This decrease in *Lin28b* coincides with accumulation of mature *let-7* microRNAs, whose biogenesis is regulated by Lin28 proteins. We find that inhibition of *let-7* in the adult hematopoietic system recapitulates fetal erythroid-dominant hematopoiesis. Conversely, deletion of *Lin28b* or ectopic activation of *let-7* microRNAs in the fetal state induces a shift toward adult-like myeloid-dominant output. Furthermore, we identify Hmga2 as an effector of this genetic switch. These studies provide the first detailed analysis of the roles of endogenous *Lin28b* and *let-7* in the timing of hematopoietic states during development.

Hematopoiesis is a tightly controlled process in which stem and progenitor cells generate mature progeny to maintain a dynamic complement of blood cells that together support the physiological needs of oxygen transport, immune competence, and hemostasis. Hematopoietic stem cells (HSCs) produce common myeloid progenitors (CMPs) that commit to either granulocyte–monocyte progenitors (GMPs) or megakaryocyte–erythroid progenitors (MEPs), which further differentiate into mature cells, possibly by acquisition of transcriptional priming that confers ultimate lineage fate (Akashi et al., 2000; Traver et al., 2001; Paul et al., 2015). Situations of stress, such as hemorrhage or systemic inflammation, can enhance erythroid or myeloid output, respectively, while maintaining an adaptable pool of myeloerythroid progenitors (Doulatov et al., 2009; Xiang et al., 2015).

During development from the fetal to adult state, the hematopoietic system undergoes controlled maturation characterized by changes in transcriptional programs (McKinney-Freeman et al., 2012) that promote reduction in HSC self-renewal (Rebel et al., 1996; Bowie et al., 2007), postnatal hemoglobin recruitment (Sankaran et al., 2010), alterations in progenitor priming (Notta et al., 2016), and lymphoid respecification (Ikuta et al., 1990; Ikuta and Weissman, 1991). Efforts to date have identified *Sox17* and Polycomb family members as key regulators of this process (He et al., 2011; Mochizuki-

*R.G. Rowe and L.D. Wang contributed equally to this paper.

Correspondence to George Q. Daley: george.daley@childrens.harvard.edu

P.T. Nguyen's present address is University of California, San Francisco, Medical School, San Francisco, CA 94143.

A. Rodriguez's present address is Dept. of Physical Therapy, University of Texas Medical Branch, Galveston, TX 77555.

Abbreviations used: BFU-E, burst-forming unit erythroid; CMP, common myeloid progenitor; FDR, false discovery rate; FL, fetal liver; GMP, granulocyte–monocyte progenitor; GSEA, gene set enrichment analysis; HSC, hematopoietic stem cell; MEP, megakaryocyte–erythroid progenitor; MPP, multipotent progenitor; qPCR, quantitative PCR.

© 2016 Rowe et al. This article is distributed under the terms of an Attribution–Noncommercial–Share Alike–No Mirror Sites license for the first six months after the publication date (see http://www.rupress.org/terms). After six months it is available under a Creative Commons License (Attribution–Noncommercial–Share Alike 3.0 Unported license, as described at http://creativecommons.org/licenses/by-nc-sa/3.0/).

The Rockefeller University Press $30.00
J. Exp. Med. 2016 Vol. 213 No. 8 1497–1512
www.jem.org/cgi/doi/10.1084/jem.20151912

The Journal of Experimental Medicine

Downloaded from http://rupress.org/jem/article-pdf/213/8/1497/1755526/jem_20151912.pdf by guest on 02 December 2025

Kashio et al., 2011; Xie et al., 2014). These findings illustrate the broader concept of developmental timing of organogenesis, whereby tissues must undergo controlled maturation so that their specialized functions dovetail with organism morphogenesis. Recently, the Lin28b RNA-binding protein has been implicated in the developmental stage–specific regulation of hematopoiesis, with its expression confined to fetal hematopoietic tissues in vivo (Yuan et al., 2012; Copley et al., 2013). Ectopic expression of *Lin28b* in adult hematopoietic tissues confers fetal-like lymphoid differentiation (Yuan et al., 2012; Zhou et al., 2015), induces fetal globin expression (Lee et al., 2013), and promotes fetal-like self-renewal capabilities in HSCs (Copley et al., 2013). To date, experiments documenting the regulation of developmental hematopoiesis by Lin28b have relied on ectopic overexpression, whereas efforts that probe the effect of loss of endogenous *Lin28b* are lacking.

LIN28A and LIN28B are RNA-binding proteins that suppress the maturation of the *let-7* family of microRNAs and modulate the translation of several mRNAs (Viswanathan et al., 2008; Shyh-Chang and Daley, 2013). Initially identified as regulators of developmental timing in *Caenorhabditis elegans* (Ambros and Horvitz, 1984; Moss et al., 1997), recent attention has focused on the capacity of LIN28 proteins to participate in the induction of pluripotency in somatic cells (Yu et al., 2007; Hanna et al., 2009) and to contribute to oncogenesis through regulation of *let-7* levels (Viswanathan et al., 2009; West et al., 2009; Jiang et al., 2012; Rao et al., 2012; Urbach et al., 2014; Wang et al., 2015; Wu et al., 2015). The mechanisms by which the Lin28–*let-7* axis projects its influence on such diverse pathophysiologic processes are beginning to come to light (Shyh-Chang and Daley, 2013). An emerging body of evidence posits a model wherein the presence of LIN28A/B is associated with a pluripotent, dedifferentiated phenotype, whereas accumulation of mature *let-7* occurs secondary to LIN28A/B down-regulation to drive terminal differentiation (Viswanathan and Daley, 2010). Given their roles in developmental timing and stem cell function, we hypothesized that the Lin28–*let-7* axis regulates myeloerythroid progenitor activity during development.

RESULTS

Maturation of the myeloerythroid compartment

We examined the WT mouse myeloerythroid compartment at various stages of definitive hematopoiesis ranging from the E14.5 fetal liver (FL) to the mature BM, first assessing CMP, MEP, and GMP populations (Fig. 1 A). Compared with adult BM, numbers of MEPs in E14.5 FL were sixfold higher than GMPs, a ratio that switched with time to GMP predominance in adult mice (Fig. 1, A and B). By querying granulocyte populations at different stages (Sakamoto et al., 2000), we observed a progressive increase in mature granulocytes with time, paralleling the increase in GMPs (Fig. 1, C and D). We also delineated stages of erythroid development over time (Socolovsky et al., 2001). Compared with adult BM, we found more $Ter119^+$-maturing erythroid cells in E14.5 FL, as well as a larger $CD71^+/Ter119^-$ population containing early proerythroblasts (Fig. 1, E and F). Next, we cultured FL and BM mononuclear cells in methylcellulose with myeloerythropoietic growth factors and monitored hematopoietic colony formation. We observed a larger proportion of erythroid colonies in the FL compared with the BM, with more granulocytic colonies arising from BM cells (Fig. 1 G). Finally, as the CMP population is thought to differentiate to either MEPs or GMPs, we analyzed CMP transcriptome profiles by whole RNA sequencing (RNAseq; $n = 3$ biological replicates for each condition). A comparison with published datasets (Wong et al., 2013; Wu et al., 2014) revealed that transcripts specific to BM CMPs are enriched in myeloid lineage–specific transcripts (relative to erythroblasts), whereas transcripts specific to FL CMPs are enriched in erythroblast-specific transcripts (Fig. 2 A). Consistent with this finding, CMPs from BM contained a significantly higher expression of myeloid-specific genes, including *Elane*, *Mmp8*, *Ctsg*, *Mmp9*, *Ngp*, and *Ltf*, whereas FL CMPs expressed higher levels of the platelet/erythroid factors *Rcor2*, *Ptsg1/Cox1*, and *P2ry12* (Fig. 2 B). Collectively, these data demonstrate that MEPs and their differentiated progeny predominate in the E14.5 FL compared with BM, in which GMPs and granulocytes predominate, possibly because of transcriptional priming of lineage commitment of CMPs, and describe normal developmental maturation within the myeloerythroid compartment.

Levels of *Lin28b* decrease, whereas *let-7* species increase in myeloid progenitors during development

Using RNAseq, we found that a total of 1,081 genes were higher and 1,636 genes were lower in E14.5 FL CMPs compared with BM CMPs at a significance cutoff of 0.001 (Table S1). *Lin28b* was the second most significantly enriched transcript in the FL, which we confirmed by quantitative PCR (qPCR; Fig. 3 A). We noted enrichment of known *let-7* target mRNAs in FL CMPs, suggesting that FL CMPs contain lower overall *let-7* levels, possibly as a consequence of relatively higher levels of *Lin28b* compared with BM CMPs (Fig. 3 B). Therefore, we examined developmental distribution of mature *let7* forms and observed significantly higher levels of several mature *let-7* microRNAs in adult BM CMPs compared with FL CMPs (Fig. 3 C). Because both transcriptional and posttranscriptional mechanisms govern *let-7* levels, we measured levels of pre– and pri–*let-7* in FL and BM CMPs, as well as levels of a *let-7* host gene. We observed significantly higher levels of several *let-7* precursors as well as the host gene for pre–*let-7b* and pre–*let-7c2* in adult BM compared with FL CMPs (Fig. 3, D and E). Together, these data support the notion that *let-7* accumulates in CMPs with hematopoietic maturation.

Suppression of *let-7* activity in the adult confers an FL-like myeloerythropoietic phenotype

Because several mature *let-7* species are present at higher levels in adult CMPs relative to FL CMPs, we endeavored to

Downloaded from http://rupress.org/jem/article-pdf/213/8/1497/1755526/jem_20151912.pdf by guest on 02 December 2025

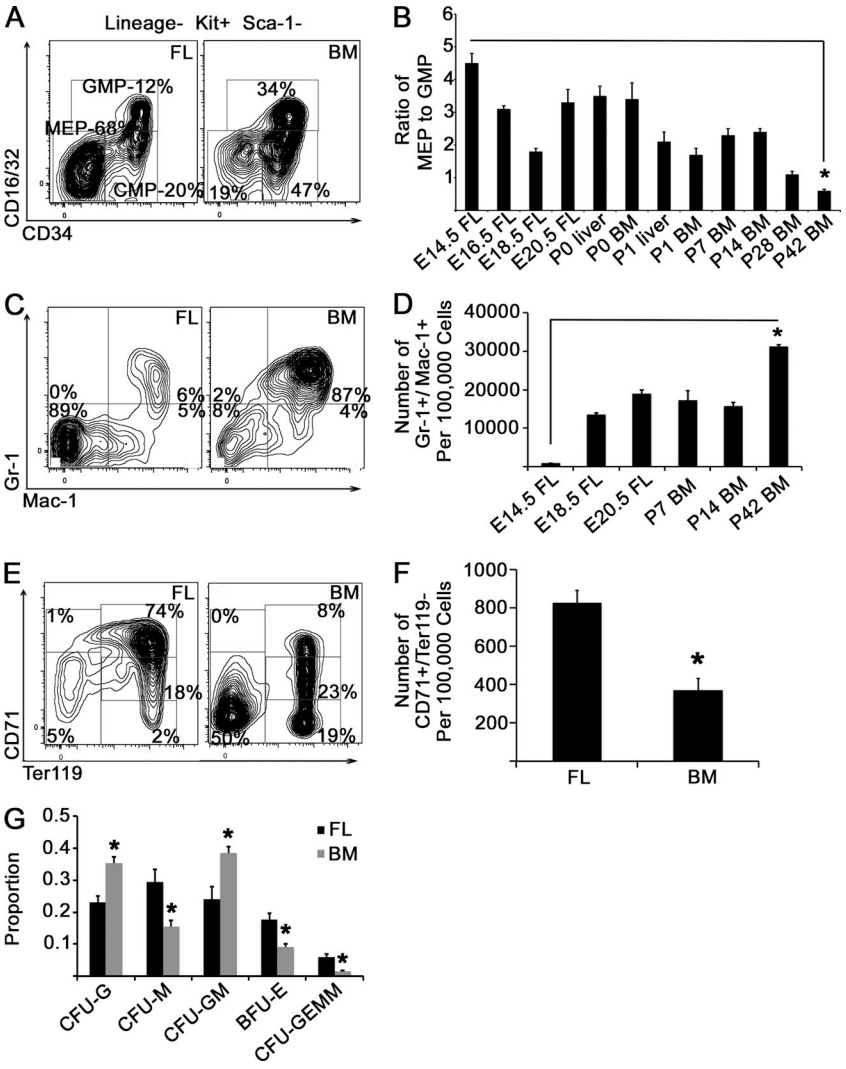

Figure 1. **Myeloerythroid development.** (A) Whole WT FL mononuclear cells or BM cells were gated on viable, lineage$^-$, c-kit$^+$, and Sca-1$^-$ cells, and representative staining patterns for CD16/32 and CD34 are presented. MEPs are defined as lineage$^-$, c-kit$^+$, Sca-1$^-$, CD16/32$^-$, and CD34$^-$; GMPs are defined as lineage$^-$, c-kit$^+$, Sca-1$^-$, CD16/32^{hi}, and CD34$^+$; and CMPs are defined as lineage$^-$, c-kit$^+$, Sca-1$^-$, CD16/32^{lo}, and CD34$^+$. (B) FL or BM cells were isolated at the indicated time points, and the ratio of MEPs to GMPs is presented. *, $P < 0.0001$ by Student's *t* test, comparing E14.5 FL and P42 BM time points. $n = 6$ animals for each time point over two experiments. (C) BM or FL cells were stained with the indicated antibodies (including erythroid and lymphoid lineage antibodies), and representative flow cytometry plots are presented. (D) FL or adult BM mononuclear cells were isolated at the indicated developmental time points, and the number of Gr-1$^+$/Mac-1$^+$ cells per 100,000 cells is presented. *, $P < 0.001$ by Student's *t* test for E14.5 FL and P42 BM time points. $n = 6$ animals over two experiments. (E) FL or BM cells were stained with antibodies against Ter119 and CD71, and representative flow cytometry plots are presented. (F) The number of CD71$^+$/Ter119$^-$ cells in FL versus adult BM is presented. *, $P < 0.0001$ by Student's *t* test. $n = 6$ animals over two experiments. (G) Mononuclear cells were cultured in methylcellulose for 14 d in the presence of growth factors (stem cell factor, IL-3, IL-6, and erythropoietin). Colonies were scored by morphology, and the proportion of each colony type in the cultures is presented. *, $P < 0.05$ for each colony type by Student's *t* test. $n = 4$ adult BM and 6 E14.5 FL over two experiments. Error bars represent SEM. CFU-M, CFU monocyte; CFU-G, CFU granulocyte; CFU-GM, CFU granulocyte–monocyte.

inhibit *let-7* activity in the adult and assess effects on myeloerythropoiesis. To this end, we used three complementary tools: (1) ectopic overexpression of *LIN28B* to impair maturation of *let-7* precursors, (2) expression of a pan–*let-7* sponge in BM CMPs to functionally sequester mature *let-7* species from their endogenous mRNA targets, and (3) use of a mouse model deficient for the polycistronic transcript encoding *let-7b* (the *let-7* form most enriched in BM CMPs compared with FL CMPs) and *let-7c2*.

We first used a mouse model of doxycycline-induced human *LIN28B* expression (*iLIN28B* mice; Shyh-Chang et al., 2013). 14 d of doxycycline exposure achieved a robust induction of LIN28B in BM cells (Fig. 4 A), suppression of several mature *let-7* species (Fig. 4 B), as well as a decrease in GMPs and an FL-like increase in MEPs in the BM (Fig. 4, C and D) compared with unexposed *iLIN28B* mice. *LIN28B*-expressing adult hematopoietic tissues were generally more proliferative than control tissues by Ki67 staining (not depicted), but we did not observe obvious differences in overall tissue cellularity or differences in the rates of CMP proliferation or apoptosis as measured by in vivo bromodeoxyuridine incorporation and annexin V staining between *iLIN28B* and control mice (control 21.9 ± 5.5% compared with *iLIN28B* 25.9 ± 5.7% bromodeoxyuridine-positive CMPs after a 4-h in vivo pulse [$P = 0.63$]; control 20.5 ± 3.4% compared with *iLIN28B* 27.0 ± 4% annexin V–positive CMPs in vivo [$P = 0.25$]; $n = 5$ control and *iLIN28B* mice across three independent experiments for both assays; both analyses by Student's *t* test). *LIN28B* induction resulted in increased numbers of Ter119-positive committed erythroid cells (as well as CD71$^+$/Ter119$^-$ early erythroblasts, similar to E14.5 FL) and decreased numbers of mature BM granulocytes compared with controls (Fig. 4, E–H). By morphology, we observed more erythroblasts with fewer mature neutrophils in the BM (Fig. 4 I) and expansion of the splenic red pulp (Fig. 4 J) in doxycycline-exposed *TRE-LIN28B* mice compared with unexposed mice. We cultured *iLIN28B* BM cells in methylcellulose with myeloerythropoietic growth factors

Downloaded from http://rupress.org/jem/article-pdf/213/8/1497/1755526/jem_20151912.pdf by guest on 02 December 2025

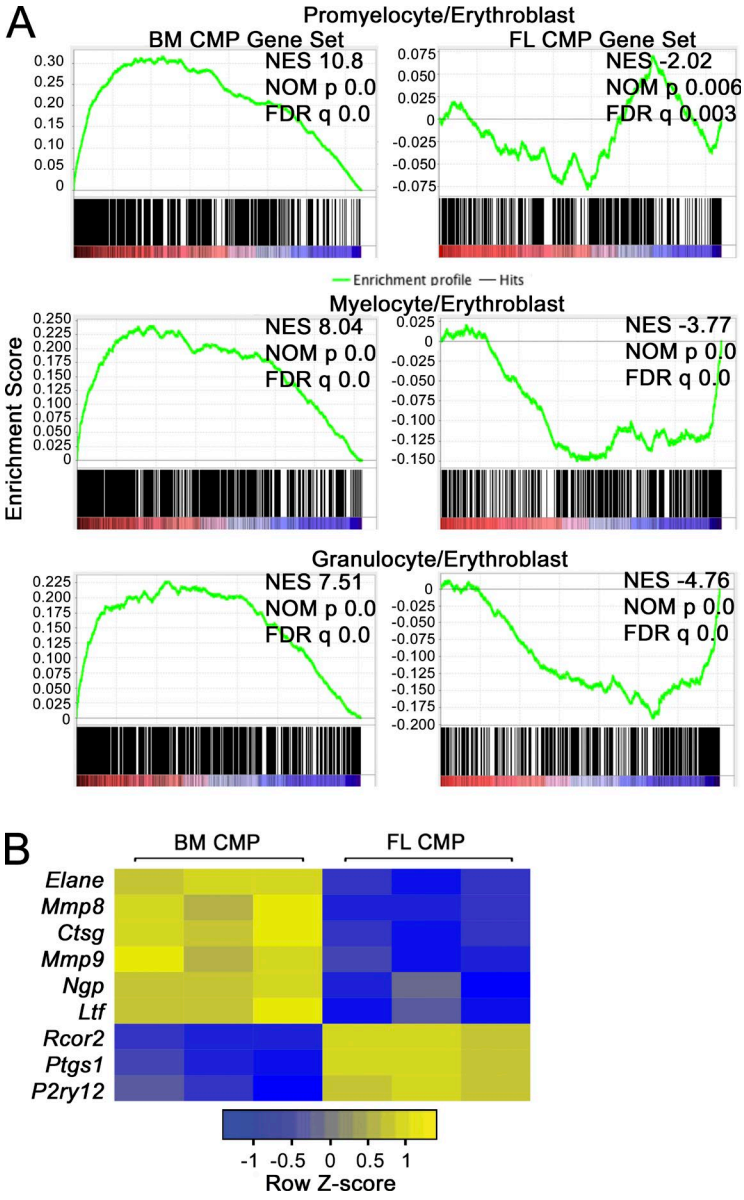

Figure 2. **RNAseq analysis of CMPs.** (A) FL and adult BM CMPs (n = 3 biological replicates for each condition isolated over at least two separate sorting experiments) were compared by RNAseq to identify significantly different genes between the two populations at a false discovery rate (FDR) cutoff of <0.001. GSEA was performed to compare adult BM CMP- and FL CMP-specific transcripts to normal adult promyelocyte, myelocyte, granulocyte, and erythroblast transcriptomes. In the top row, a significant positive correlation was observed between adult BM CMP-specific transcripts and promyelocyte-enriched transcripts (left), indicating enrichment of adult BM CMP-specific transcripts among transcripts increased in promyelocytes relative to erythroblasts. A significant negative correlation was observed between FL CMP-specific transcripts (right) and transcripts increased in promyelocytes relative to erythroblasts, indicating correlation with erythroblast-specific transcripts. Normalized enrichment score (NES), nominal p-value (NOM p), and FDR are presented. The same analysis was performed in the middle with myelocyte transcripts and at the bottom with granulocyte transcripts. (B) Heat maps showing expression of erythroid/platelet-specific and granulocyte/monocyte-specific transcripts measured by RNAseq are presented.

and observed increased erythroid colony forming activity in *LIN28B*-induced cells, analogous to WT FL-derived cultures (compare Fig. 4 K with Fig. 1 G). Competitive transplantation of *iLIN28B* HSCs with WT cells (Fig. 5, A and B) as well as a hematopoietic-specific *LIN28B* ectopic expression model showed similar effects on myeloid progenitors (Fig. 5, C–I).

Our second method of interfering with *let-7* function in adult myeloerythropoiesis was introduction of a *let-7* sponge construct in sorted BM CMPs (Kumar et al., 2008), followed by culture of the sponge- or empty vector–transduced BM CMPs in methylcellulose in the presence of growth factors. Sequestration of *let-7* resulted in significantly increased proportions of burst-forming unit erythroid (BFU-E) colonies and mRNA levels of mouse globin genes compared with control cells in culture (Fig. 6, A and B). Third, we analyzed the myeloerythroid progenitor compartment of a strain of mice bearing a deletion of the *let-7b* and *let-7c2* polycistronic host gene (*let-7* KO) and observed a trend toward decreased GMPs and increased MEPs (Fig. 6, C and D), as well as fewer BM granulocytes compared with WT isogenic controls (Fig. 6, E and F), but not a significant effect on erythroid maturation or distribution of myeloerythroid colony formation in vitro (not depicted), potentially because of compensatory effects of other *let-7* species in this model.

Activation of *let-7g* in the FL drives an adult BM-like myeloerythroid phenotype

If *let-7* function specifies adult BM myeloerythropoiesis, we hypothesized that mistimed ectopic activation of *let-7* in the FL would result in an aberrant adult-like myeloeryth-

Downloaded from http://rupress.org/jem/article-pdf/213/8/1497/1755526/jem_20151912.pdf by guest on 02 December 2025

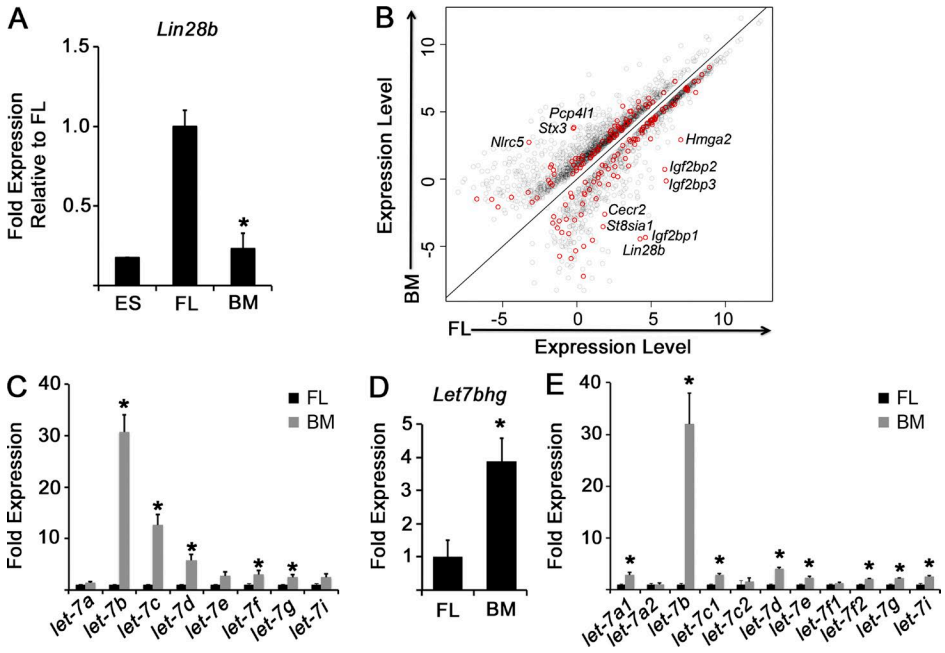

Figure 3. **The *Lin28–let-7* axis during myeloerythropoiesis.** (A) FL or adult BM CMPs were isolated by FACS. The level of *Lin28b* mRNA was measured by qPCR in E14.5 FL or BM CMPs, and the levels were compared with mouse embryonic stem (ES) cells by qPCR. *, $P < 0.0001$ by Student's *t* test. $n = 6$ replicates for FL and BM each over two experiments. An 8.08-fold expression increase in *Lin28b* was observed in FL CMPs compared with adult BM CMPs; $P = 2.34 \times 10^{-15}$ by RNAseq. (B) Scatter plot of differentially expressed genes between FL and adult BM CMPs as measured by RNAseq. Predicted *let-7* targets with significantly different expression between FL and adult BM CMPs at an FDR of 0.001 are indicated in red. Pertinent transcripts are denoted. $n = 3$ biological replicates over at least two separate sorting experiments for BM and FL. (C–E) Levels of the indicated mature *let-7* microRNA family members (C), *Let7bhg* (D), or *let-7* precursors (E) were measured by qPCR in FACS-sorted FL or adult BM CMPs. The results are presented as fold expression compared with FL, normalized to an expression value of 1. *, $P < 0.05$. $n = 6$ embryos/mice sorted from three independent experiments. Error bars represent SEM.

roid phenotype. To this end, we used a mouse strain wherein expression of a Lin28-resistant chimeric form of *let-7g* (*let-7S21L*) is induced by doxycycline exposure (*iLet-7* mouse; Zhu et al., 2011) and assessed myeloerythroid colony formation in E14.5 FL-derived cells from *iLet-7* embryos and controls after 2–4 d of in utero induction before harvesting of embryos. Induction of *let-7S21L* resulted in an increased proportion of CFU granulocyte colonies at the expense of BFU-E and CFU-GEMM (granulocyte, erythrocyte, monocyte, and megakaryocyte) colonies (Fig. 7 A). To assess effects of ectopic *let-7* in vivo, we induced females bearing mixed litters of *iLet-7* embryos and littermate controls at E10.5 with doxycycline in the drinking water, which resulted in robust *let-7g* expression in the FL when harvested at E14.5 (Fig. 7 B). Although many *iLet-7* embryos died, analysis of myeloid progenitors in viable embryos at E14.5 revealed depletion of MEPs (Fig. 7, C and D), a trend toward increased FL granulocytes (Fig. 7, E and F), and diminished numbers of $CD71^{+}/Ter119^{-}$ early erythroid progenitors with an adult-like pattern of erythroid differentiation (Fig. 7, G and H).

Endogenous *Lin28b* deficiency alters the myeloid progenitor pool in the FL

Because *Lin28b* decreases during myeloerythroid maturation and ectopic LIN28B drives an FL-like myeloerythroid phenotype in BM CMPs, we examined the progenitor pool in *Lin28b*-deficient E14.5 FLs and observed an increased number of GMPs in *Lin28b*-deficient embryos compared with littermate controls (Fig. 8, A and B). Although we did not observe a significant phenotype related to erythroid maturation (not depicted), we did find increased numbers of granulocytes in the FLs of *Lin28b*-deficient embryos compared with WT littermates (Fig. 8, C and D). Culture of FL mononuclear cells in methylcellulose with growth factors did not demonstrate a significant difference in colony formation between genotypes (not depicted). Importantly, we did not observe a compensatory up-regulation of *Lin28a* in *Lin28b*-deficient FLs (not depicted). Consistent with a fetal-specific role for *Lin28b* in myelopoiesis, complete blood counts in adult *Lin28b*-deficient mice were similar to control mice, with the exception of a mild anemia in the null mice (not depicted). We hypothesized that the incomplete induction of an adult BM-like myelopoietic phenotype in *Lin28b*-deficient embryos might be caused by a relative paucity of precursor *let-7* species in FL CMPs compared with adult BM CMPs (Fig. 3 C). Therefore, we assessed the ability of *Lin28b*-deficient E14.5 CMPs to form mature *let-7* microRNAs. In the absence of Lin28b, we observed an increase in a subset of mature *let-7* forms in FL CMPs (*let-7d*, *let-7g*, and *let-7i*); however, levels of *let-7* were still lower than those observed during physiological myelo-

Downloaded from http://rupress.org/jem/article-pdf/213/8/1497/1755526/jem_20151912.pdf by guest on 02 December 2025

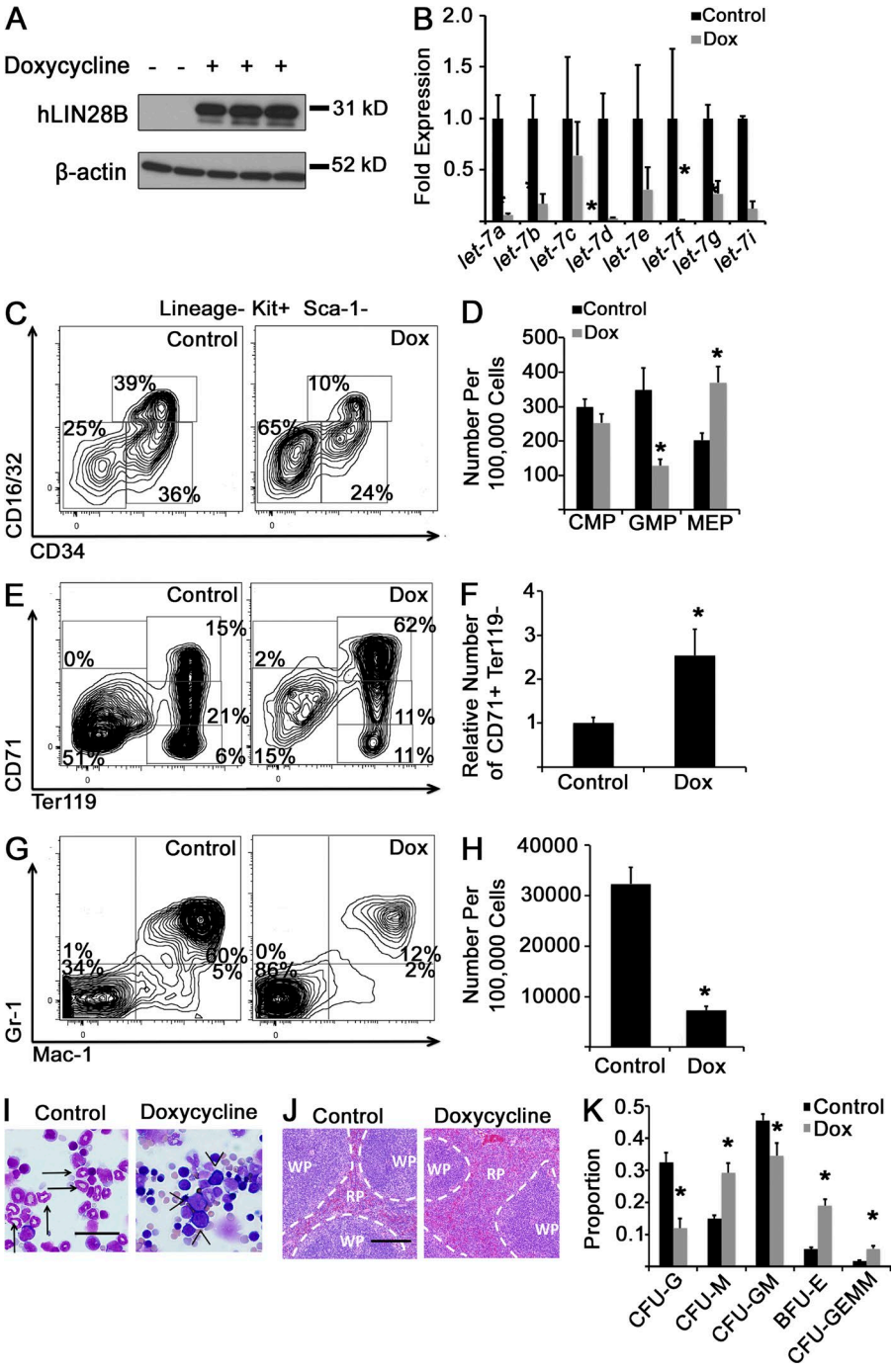

Figure 4. **Activation of *LIN28B* in adult BM.** (A) Adult *iLIN28B* mice were exposed to 1 g/liter doxycycline in drinking water or standard water for 14 d, at which time BM mononuclear cells were isolated, and Western blot analysis for human LIN28B was performed. (B) RNA was isolated from BM CMPs with and without doxycycline (Dox) exposure, and levels of mature *let-7* microRNAs were measured by qPCR. For each *let-7* form, results are normalized to the control, nondoxycycline-exposed condition. *, $P < 0.05$ by Student's *t* test. $n = 4$ uninduced and 5 doxycycline-exposed across three experiments. (C) BM mononuclear cells from adult *iLIN28B* mice with and without 14 d of doxycycline exposure were isolated and immunostained, with representative flow cytometry plots presented. (D) Numbers of myeloid progenitor cells per 100,000 BM mononuclear cells are shown. *, $P < 0.01$ by Student's *t* test. (E) Whole BM cells were analyzed for red blood cell progenitor populations by flow cytometry. Representative plots are shown. (F) Numbers of $CD71^+/Ter119^-$ cells in doxycycline-exposed *iLIN28B* animals relative to the control are shown. *, $P < 0.02$ by Student's *t* test. (G) BM mononuclear cells under the indicated conditions were immunostained for Gr-1 and Mac-1. Representative flow cytometry plots are shown. (H) Numbers of $Gr\text{-}1^+/Mac\text{-}1^+$ mature granulocytes per 100,000 BM mononuclear cells under the indicated conditions are presented. *, $P < 0.0001$ by Student's *t* test. (D, F, and H) $n = 8$ mice for the control condition and 7 mice for the doxycycline-exposed condition across three experiments. (I and J) Morphology of BM cells (I) or splenic tissue (J) from control or doxycycline-treated *iLIN28B* mice is shown. Images are representative of specimens obtained over at least three independent experiments. (I) Bar, 40 µm. Arrows, neutrophils; arrowheads, erythroblasts. (J) Bar, 200 µm. RP, red pulp; WP, white pulp. Dashed lines indicate borders of these two splenic tissues. (K) BM mononuclear cells from *iLIN28B* mice exposed to doxycycline for 14 d or unexposed mice were cultured in methylcellulose in the presence of growth factors. After 14 d of culture, colony morphology was scored, and the mean proportions of each colony type are presented. *, $P < 0.05$ by Student's *t* test comparing each colony type. $n = 5$ control mice and 4 doxycycline-treated mice across three experiments. Error bars represent SEM. CFU-M, CFU monocyte; CFU-G, CFU granulocyte; CFU-GM, CFU granulocyte–monocyte.

Downloaded from http://rupress.org/jem/article-pdf/213/8/1497/1755526/jem_20151912.pdf by guest on 02 December 2025

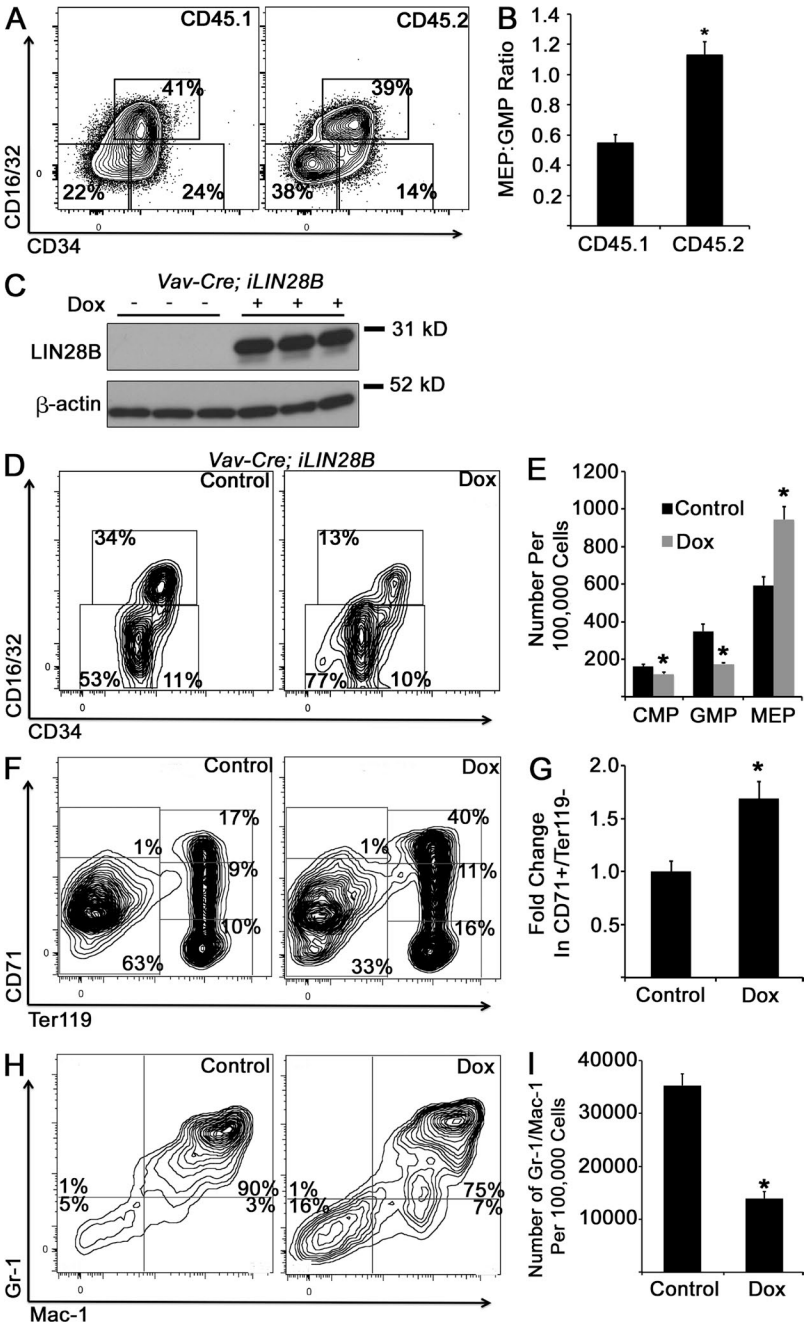

Figure 5. **Transplantation of *iLIN28B* BM into WT recipients and tissue-specific LIN28B induction.** (A) Lineage$^-$, c-kit$^+$, Sca-1$^+$, CD150$^+$, and CD48$^-$ long-term HSCs were purified by FACS from BM of *iLIN28B* mice (CD45.2) exposed to doxycycline. Long-term HSCs were cotransplanted with CD45.1 BM cells into lethally irradiated CD45.1 recipient mice. Recipient mice continued to receive doxycycline in their drinking water and were sacrificed 16–20 wk after transplantation, and myeloid progenitors in the BM were analyzed within the CD45.1 and CD45.2 fractions. Representative flow cytometry plots are shown. (B) Ratio of MEP to GMP in the CD45.1 and CD45.2 fractions in mixed chimeric recipient mice is presented. *, $P < 0.0001$ by Student's *t* test. $n = 10$ mice. (C) Triple transgenic mice carrying alleles for *iLIN28B*, the reverse tetracycline transactivator (rtta) downstream of a loxp-flanked stop codon cassette, and *Vav1*-cre for hematopoietic-specific excision of the loxp-flanked stop cassette and hematopoietic-specific expression of rtta and transcription of the *iLIN28B* transgene in the presence of doxycycline. Exposure of triple transgenic mice to doxycycline (Dox) for 14 d resulted in robust LIN28B induction in the adult BM as assessed by Western blotting. (D and E) Myeloid progenitor profiles were assessed after 14 d of doxycycline exposure in triple transgenic mice compared with unexposed mice. *, $P < 0.05$ by Student's *t* test. (F and G) BM cells were stained for erythroid cells, and numbers of CD71$^+$/Ter119$^-$ cells were quantified. *, $P = 0.02$ by Student's *t* test. (H and I) BM cells were stained to assess granulocyte maturation, and numbers of Gr-1$^+$/Mac-1$^+$ cells were quantified. *, $P = 0.001$ by Student's *t* test. (D–I) $n = 3$ mice across two experiments for each condition. Error bars represent SEM.

erythroid maturation (compare Fig. 8 E with Fig. 3 C). Thus, it is likely that the consequences of loss of *Lin28b* in the FL are mitigated by an inability to generate adult BM-like levels of *let-7* microRNAs, possibly caused by low levels of basal transcription of *let-7* precursors.

Transcriptional programs underlying *Lin28b/let-7* control of myeloerythropoiesis

We performed RNAseq on CMPs isolated from WT FL, WT adult BM, *Lin28b*-deficient FL, and *iLIN28B* adult BM. The numbers of differentially expressed genes between relevant comparisons are shown in Fig. 9 A. We observed significant enrichment of *let-7* target genes in three comparisons (Fig. 9 B), in patterns consistent with the relative *let-7* abundance across development described above (Fig. 3 C). Gene set enrichment analysis (GSEA) revealed that mRNAs affected by LIN28B induction in adult BM CMPs had a highly significant coordinate pattern of regulation with those altered during normal development from FL to BM myeloerythropoiesis (Fig. 9 C). As such, we compared the sets of mRNAs altered in FL CMPs and *iLIN28B* BM CMPs relative to WT BM CMPs and noted a significant degree of overlap (Fig. 9 D).

Downloaded from http://rupress.org/jem/article-pdf/213/8/1497/1755526/jem_20151912.pdf by guest on 02 December 2025

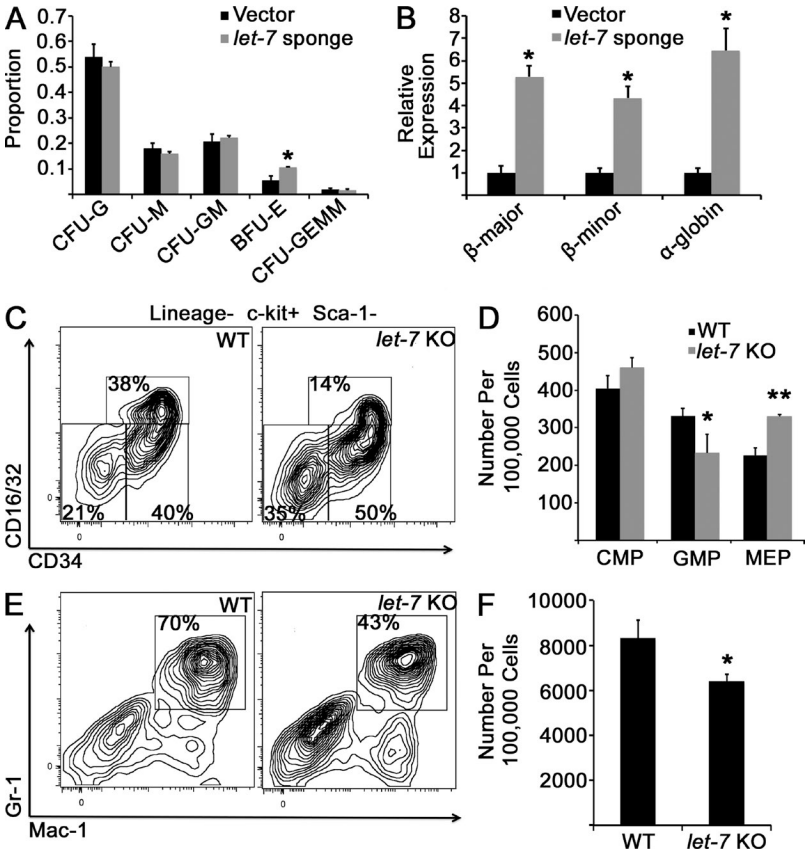

Figure 6. **Inhibition of *let-7* in adult myeloerythropoiesis.** (A) Purified WT adult BM CMPs were retrovirally transduced with an empty vector or a *let-7* sponge construct and cultured in methylcellulose for 14 d, when colonies were scored by morphology. Colony distributions are presented. *, P = 0.03 by Student's *t* test. *n* = 5 replicates for vector and sponge constructs across three independent experiments. CFU-M, CFU monocyte; CFU-G, CFU granulocyte; CFU-GM, CFU granulocyte–monocyte. (B) RNA was isolated from cultures after 14 d, and levels of mouse globin genes were measured by qPCR. *, P < 0.01 by Student's *t* test. *n* = 3 replicates across three experiments. (C) Adult mice with the locus encoding *let-7b1* and *let-7c2*–deleted (*let-7* KO) or WT C57 littermates were euthanized, BM cells were stained with the indicated antibodies, and myeloid progenitor populations were analyzed by flow cytometry. (D) Numbers of myeloid progenitor cells are presented. *, P = 0.14; **, P = 0.009 by Student's *t* test for each comparison. *n* = 3 WT and *let-7* KO mice analyzed; results are representative of two experiments performed (a separate experiment was performed with mice of strain 129 with similar results). (E) BM from the indicated mice was isolated and stained with the indicated antibodies to evaluate granulocyte populations. (F) Numbers of Gr-1$^+$/Mac-1$^+$ mature granulocytes are presented. *, P = 0.09 by Student's *t* test. *n* = 3 for each genotype; the phenotype is verified in an independent strain in an independent experiment. Error bars represent SEM.

On the list of commonly regulated mRNAs, we found several markers of mature neutrophils (*Ctsg* and *Slpi*) and monocytes (*Matb* and *Spic*) that were more abundant in WT BM compared with *iLIN28B* BM and WT FLs (Fig. 9 E). Among the commonly enriched transcripts in FL CMPs and *iLIN28B* BM CMPs, 16/61 (26%) had predicted *let-7* binding sites, whereas among the transcripts that were commonly lower, only 5/134 (4%) were predicted *let-7* targets. Interestingly, LIN28B induction resulted in a 4.58-fold increased expression of embryonic globin *Hbb-y* relative to WT BM CMPs.

LIN28B effect on multipotent progenitors (MPPs)

As Lin28/*let-7* appears to regulate myeloerythropoiesis at the level of the CMP, possibly via transcriptional priming, we assessed the myeloerythroid differentiation potential of MPPs—which give rise to CMPs in hematopoietic ontogeny—in *iLIN28B* and control mice. Within the LSK (Lineage$^-$, Sca-1$^+$, c-kit$^+$) compartment, we resolved MPP and long-term and short-term HSC populations, defining MPPs as CD150$^-$ and CD48$^{-/low}$ (Fig. 10 A; Oguro et al., 2013). We did not observe differences in MPP frequency between *iLIN28B* and control BM (Fig. 10 B). MPPs were sorted and cultured in methylcellulose in the presence of myelopoietic cytokines, and colonies were scored by morphology after 10–14 d. We did not observe differences in colony distribution, save for restraint of full CFU granulocyte potential by ectopic LIN28B expression, and no effect on erythroid differentiation (Fig. 10 C), consistent with an effect on myeloerythroid differentiation mediated predominantly at the CMP level.

Hmga2 as an effector of Lin28b–*let-7*–controlled myeloerythropoiesis

By RNAseq, the *let-7* target gene *Hmga2* (Copley et al., 2013) was one of the most significantly increased mRNAs in both *iLIN28B* CMPs and FL CMPs compared with adult BM CMPs (Fig. 9 E). We confirmed this differential expression by qPCR (Fig. 10 D). Moreover, we found lower levels of *Hmga2* in *Lin28b*-deficient FL CMPs (Fig. 10 E). Because *Hmga2* is a well-known hematopoietic regulator (Ikeda et al., 2011; Lam et al., 2014), we isolated adult BM CMPs and ectopically expressed a mouse *Hmga2* transgene or a control vector and cultured the CMPs in methylcellulose with hematopoietic growth factors for 14 d. Expression of ectopic *Hmga2* resulted in an increased proportion of BFU-E colonies relative to control cultures after 14 d (Fig. 10 F), paralleling an FL-like phenotype and indicating that Hmga2 is a mediator of the effect of the Lin28–*let-7* axis on hematopoietic maturation.

DISCUSSION

Hematopoiesis is a tightly regulated but adaptable process in which production of terminally differentiated cells responds

Downloaded from http://rupress.org/jem/article-pdf/213/8/1497/1755526/jem_20151912.pdf by guest on 02 December 2025

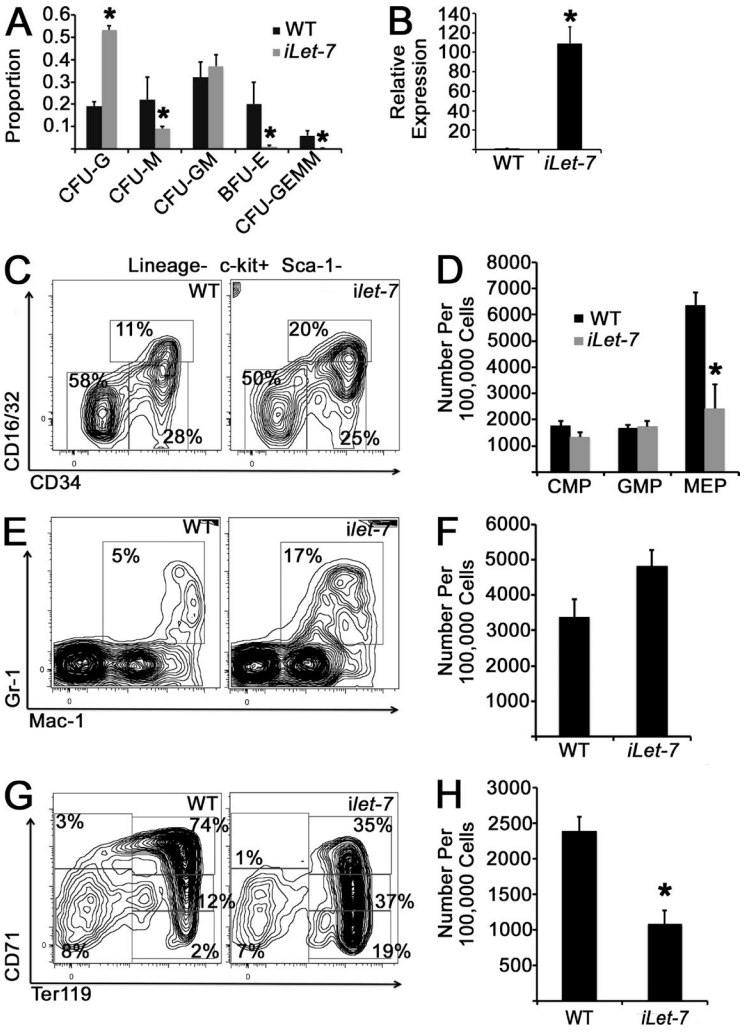

Figure 7. **Induction of *let-7* in FL hematopoietic cells.** (A) Pregnant females carrying *iLet-7* embryos and littermate controls were exposed to doxycycline for 2–4 d before harvesting at E14.5. FL mononuclear cells were cultured in methylcellulose for 14 d in the presence of doxycycline, when colony morphology was scored. Proportions of each colony type are presented. *, $P < 0.05$ by Student's *t* test for each colony type comparison. $n = 8$ control and 4 *iLet-7* embryos across three experiments. CFU-M, CFU monocyte; CFU-G, CFU granulocyte; CFU-GM, CFU granulocyte–monocyte. (B) *let-7g* induction in the FL at E14.5 after 4-d maternal doxycycline exposure as measured by qPCR. *, $P < 0.0001$ by Student's *t* test. $n = 7$ WT and 2 *iLet-7* embryos from two independent experiments. (C and D) FL cells from the indicated genotypes were stained with the indicated antibodies, and myeloid progenitor populations were analyzed by flow cytometry. Representative histograms are shown. (E and F) FL cells were stained with the indicated antibodies to assess mature granulocyte populations. $P = 0.05$ by Student's *t* test for control and *iLet-7* comparison of $Gr1^+/Mac\text{-}1^+$ cells. (G and H) Whole FL cells were stained with anti-CD71 and anti-Ter119 antibodies to analyze red blood cell progenitor populations by flow cytometry. (C–H) *, $P < 0.05$ comparing $CD71^+/Ter119^-$ cells. A total of 10 control and 8 *iLet-7* embryos were evaluated, obtained from three independent litters. Error bars represent SEM.

to pathophysiologic stimuli such as hypoxia, hemorrhage, infection, or inflammation (Orkin and Zon, 2008; Paulson et al., 2011; Takizawa et al., 2012). Basal myeloerythroid output is poised to meet specific developmental stage–specific demands, with erythroid production predominant in the FL to support growth under hypoxic conditions and granulocyte production favored in the adult BM to provide innate immunity and tissue repair capability. Candidate regulators of hematopoietic developmental maturation have begun to emerge (He et al., 2011; Mochizuki-Kashio et al., 2011; Xie et al., 2014). In this study, we document developmental maturation of myeloerythroid progenitors and link this mechanistically to regulation by the Lin28–*let-7*–Hmga2 axis, which is known to control developmental timing from worms to humans (Ambros and Horvitz, 1984; Yuan et al., 2012; Copley et al., 2013; Shyh-Chang and Daley, 2013).

Lin28 genes function in vertebrates to specify timing of kidney and germ cell development (Ambros and Horvitz, 1984; Moss et al., 1997; West et al., 2009; Urbach et al., 2014), as well as in tissue regeneration (Shyh-Chang et al., 2013) and muscle and nerve cell differentiation (Polesskaya et al., 2007; Yang et al., 2015). Recently, two studies have implicated *Lin28* in the timing of hematopoietic phenotypes during development (Yuan et al., 2012; Copley et al., 2013). Specifically, ectopic expression of *Lin28* in adult BM cells confers fetal-like HSC self-renewal properties and lymphopoietic phenotypes, indicating that ectopic *Lin28* expression may be sufficient to recapitulate prenatal hematopoietic programs (Yuan et al., 2012; Copley et al., 2013). Both of these studies were based on transcriptional analyses showing predominance of *let-7* in adult and *Lin28* in fetal hematopoietic cells (Yuan et al., 2012; Copley et al., 2013). Our study extends this paradigm to the myeloerythroid system. However, in contrast to these prior studies based exclusively on ectopic overexpression of *Lin28*, we have dissected the functionality of the *Lin28–let-7* axis in myeloerythroid differentiation by manipulating the timing of this developmental switch through both gain-of-function and loss-of-function studies of endogenous alleles in both adult and fetal scenarios, thereby confirming the role of endogenous Lin28 in regulating normal hematopoietic development. Furthermore, our findings provide a paradigm in which the function of this axis or other candidate regulators of developmental timing can be interrogated in other systems.

Downloaded from http://rupress.org/jem/article-pdf/213/8/1497/1755526/jem_20151912.pdf by guest on 02 December 2025

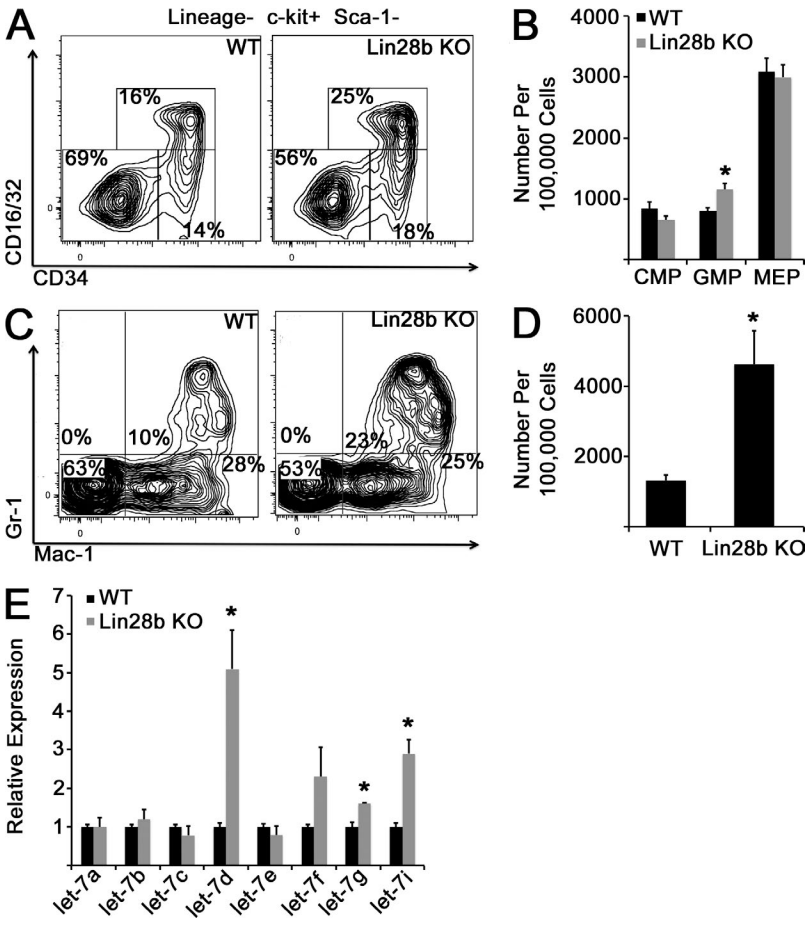

Figure 8. **Deficiency of Lin28b in the FL.** (A) WT or *Lin28b* KO embryos were isolated at E14.5, and FL cells were stained with the indicated antibodies. (B) The number of myeloid progenitor populations is shown. *, P = 0.007 by Student's *t* test. *n* = 7 WT and 6 *Lin28*-deficient embryos across three experiments. (C) FL cells of the indicated genotypes were isolated, and granulocyte populations were analyzed by flow cytometry. (D) Numbers of Gr-1$^+$/Mac-1$^+$ granulocytes per 100,000 FL mononuclear cells are shown. *, P = 0.03 by Student's *t* test. *n* = 7 WT and 5 *Lin28b*-deficient embryos across three experiments. (E) Mature *let-7* species were measured in FL CMP cells from E14.5 embryos of the indicated genotypes. *, P < 0.05 by Student's *t* test. *n* = 3 replicates for each genotype from independent litters. Error bars represent SEM.

We observed strong reduction of *Lin28b* levels and reciprocal recruitment of several mature *let-7* species during developmental maturation of CMPs from fetus to adult, as well as coordinate modulation of several *let-7*–regulated mRNAs with developmental changes in endogenous *Lin28b* and *let-7* expression. Mature *let-7* activation in the adult seemed to occur as a result of both the down-regulation of *Lin28b*—which would be expected to permit full processing of *let-7* precursors to mature forms—as well as transcriptional activation of precursor *let-7*, indicative of two levels of *let-7* regulation. Therefore, to investigate the roles of *Lin28* and *let-7* in early myeloerythroid differentiation, we used the complementary strategies of inhibition of *let-7* function in adult tissues and inappropriate *let-7* activation in the fetal state.

In the FL, wherein erythroid output predominates, mistimed activation of *let-7* activity inappropriately drives granulocyte accumulation at the expense of erythroid activity. This observation agrees with previous studies that *let-7* expression increases during terminal granulocyte differentiation (Wong et al., 2014) and that disruption of *Lin28* expression can affect granulopoiesis (Wang et al., 2015). These results also parallel studies from the leukemia literature wherein *let-7* activity has been shown to promote myeloblast differentiation (Viswanathan et al., 2009; Emmrich et al., 2013; Pelosi et al., 2013). Consistent with both transcriptional and posttranscriptional mechanisms of *let-7* regulation, *Lin28b* deficiency alone did not fully recapitulate an adult-like myeloerythroid phenotype in the FL. In the setting of low levels of endogenous precursor *let-7* transcription, there appears to be scant *let-7* precursors present for Lin28b to impair. Therefore, the blunted phenotype of *Lin28b*-deficient FLs is likely caused by a low degree of mature *let-7* accumulation, compared with that which occurs during normal myeloerythroid maturation as a consequence of the dual effects of *Lin28b* depletion and pre/pri–*let-7* transactivation.Very little is known regarding regulators of precursor *let-7* transcription, with one study implicating *HOXA10* as a transactivator of a human *let-7*–containing tricistron (Emmrich et al., 2014). It is likely that enhanced understanding of the regulation of coordinated *Lin28b* transcriptional repression and *let-7* precursor transcriptional activation will provide further insight into developmental hematopoiesis. Given the number of mRNAs deregulated by *Lin28b* deficiency in the FL, it could also be speculated that Lin28b may play a significant role in regulating mRNA stability, as has been previously reported (Polesskaya et al., 2007).

We used three methods of *let-7* inhibition in adult BM myeloerythroid progenitors: ectopic/mistimed expression of

Downloaded from http://rupress.org/jem/article-pdf/213/8/1497/1755526/jem_20151912.pdf by guest on 02 December 2025

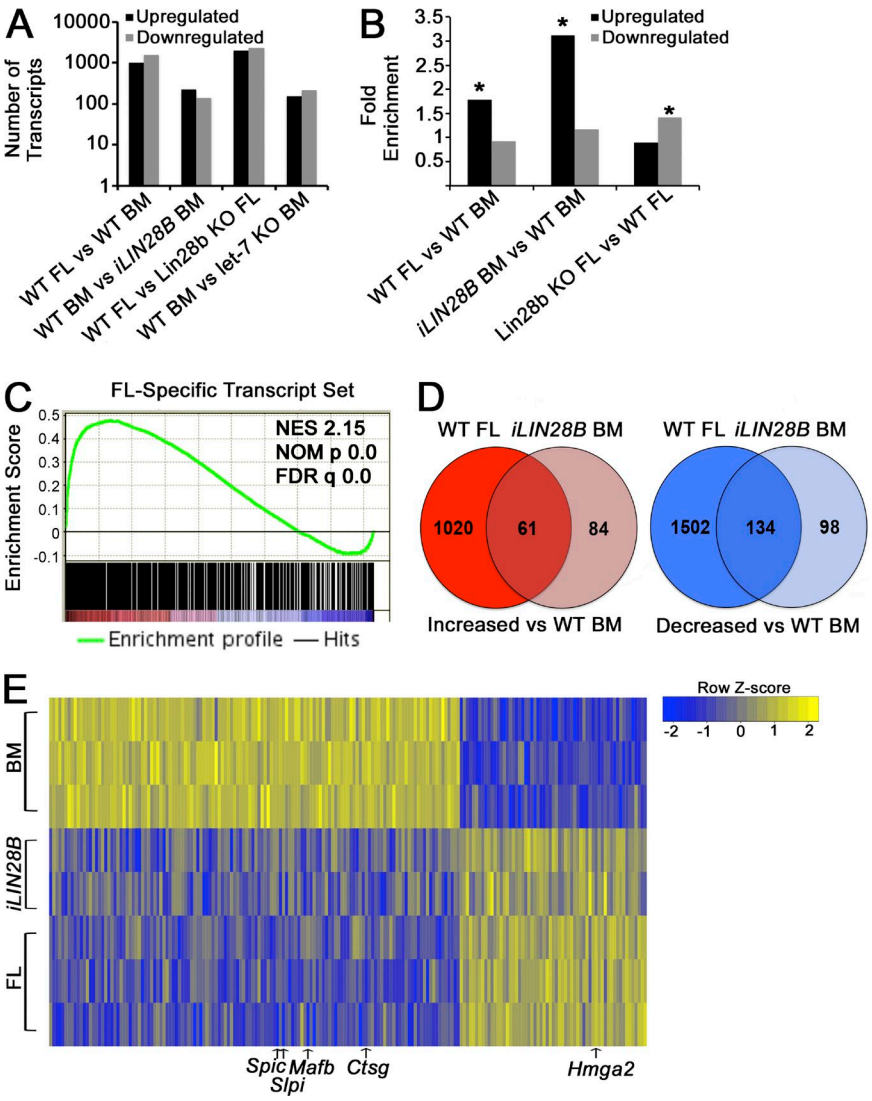

Figure 9. **Analysis of mRNA expression by RNAseq.** (A) Raw numbers of differentially expressed mRNAs for the CMP comparisons indicated are shown (FDR cutoff for significance is 0.001). (B) Fold enrichment of *let-7* target gene frequency in the indicated pools of transcripts compared with the overall frequency of *let-7* targets among all analyzed mRNAs is shown. *, $P < 0.001$; hypergeometric p-values compared with the expected frequency of *let-7* targets based on the frequency of targets among all expressed mRNAs. (C) GSEA demonstrating significant positive enrichment of the FL CMP transcriptional program in *iLIN28B* CMPs. Transcripts enriched in *iLIN28B* adult BM CMPs compared with adult BM CMPs were compared with the set of transcripts significantly enriched in WT FL CMPs compared with WT adult BM CMPs. NES, normalized enrichment score; NOM p, nominal p-value. (D) Venn diagram analysis showing overlap of transcripts up-regulated in FL CMPs and *iLIN28B* CMPs compared with WT BM CMPs (left), as well as down-regulated transcripts for these comparisons (right). The p-value for overlap of up-regulated transcripts is $<2.2 \times 10^{-16}$ (expected number of 16.22); the p-value for overlap of down-regulated transcripts is $<2.2 \times 10^{-16}$ (expected number of 39.15). Analysis was performed with Fisher's exact test. (E) Heat map demonstrating relative expression levels of the transcripts commonly up-regulated or down-regulated in *iLIN28B* CMPs and WT FL CMPs compared with WT BM CMPs. Pertinent transcripts are denoted.

LIN28B, a novel mouse model of precursor *let-7b1/c2* deficiency, and a *let-7* sponge construct. Although prior studies have suggested that ectopic *Lin28* expression in adult hematopoiesis can drive fetal-like hematopoietic output (Yuan et al., 2012; Copley et al., 2013), our findings extend this observation to the myeloerythroid system. Furthermore, our results mechanistically attribute this effect to Lin28 inhibition of *let-7* maturation, given the similar effects on myeloerythropoiesis provoked by modulating *let-7* activity directly using our *let-7* KO mice and *let-7* sponge construct. Importantly, we observed that inhibition of *let-7* directly in FACS-sorted adult BM CMPs impacted production of differentiated progeny. Together, these findings advance a mechanism by which Lin28b works at least in part via a linear axis involving control of *let-7* microRNA maturation and *let-7* target genes to specify CMP fate and cell output in the FL and adult BM. Conversely, we observed a very subtle effect of ectopic activation of LIN28B in FACS-sorted MPPs. Together with our RNAseq data, these findings suggest that transcriptional priming at the level of the CMP specifies myeloerythroid differentiation across development. Indeed, human and mouse myeloid progenitor populations possess intrinsic priming in transcriptional programs and ultimate lineage commitment at the single-cell level (Paul et al., 2015; Notta et al., 2016). Given the changes in progenitor lineage priming that occur across development (Notta et al., 2016), we propose that as heterochronic regulators of myeloerythropoiesis, Lin28b/*let-7* may play a central role in this process, a hypothesis that deserves further investigation. Finally, our genetic and transplant strategies for hematopoietic-specific *LIN28B* activation demonstrate that this effect is autonomous within the hematopoietic system.

In WT FL and adult BM, we observed varying patterns of erythroid cell differentiation from the earliest stages of MEP fate commitment through reticulocyte formation. We observed that mistimed *LIN28B* expression in the adult or

Downloaded from http://rupress.org/jem/article-pdf/213/8/1497/1755526/jem_20151912.pdf by guest on 02 December 2025

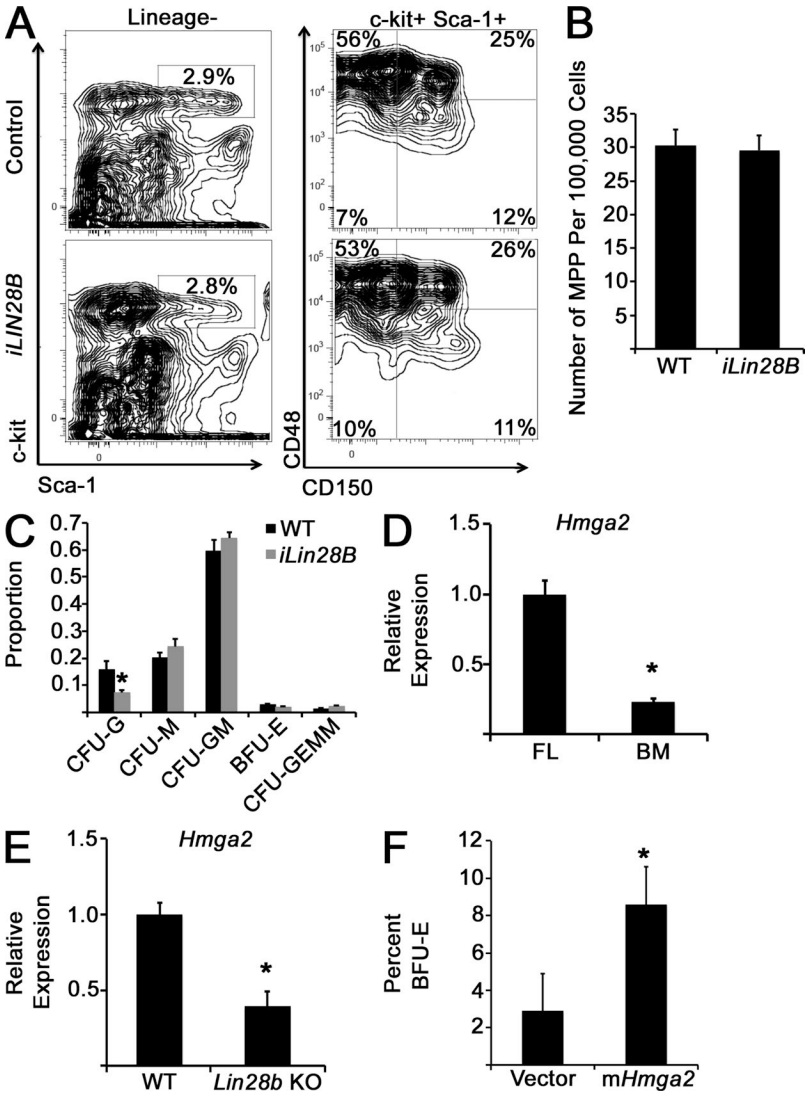

Figure 10. **Assessment of LIN28B function in MPPs and investigation of *Hmga2* as a Lin28b–*let-7* target regulating myeloerythropoiesis.** (A) Representative flow cytometry plots showing gating strategy to assess MPP populations in control and *iLIN28B* mice. (B) Numbers of MPP in the indicated mice are shown. P = 0.82 by Student's *t* test. *n* = 5 mice for each condition across three independent experiments. (C) MPPs were isolated by FACS and cultured in methylcellulose in the presence of myelopoietic cytokines for 10–14 d, when colony morphology was scored. Colony distributions are presented. *, P = 0.04 by Student's *t* test. *n* = 5 mice for each condition across three independent experiments. CFU-M, CFU monocyte; CFU-G, CFU granulocyte; CFU-GM, CFU granulocyte-monocyte. (D and E) Levels of *Hmga2* mRNA were measured by qPCR and compared in FL versus adult BM CMPs (D) or *Lin28b*-deficient compared with littermate control FL CMPs (E). (D) *, P = 0.002 by Student's *t* test. *n* = 3 in each group sorted across two experiments. (E) *, P = 0.007. *n* = 4 WT and 3 *Lin28b*-deficient samples from three separate litters. (F) WT adult BM CMPs were transduced with the indicated retroviruses and cultured in methylcellulose in the presence of growth factors for 14 d, when colony morphology was scored. The percentages of BFU-E are indicated. *, P < 0.05 by Student's *t* test. *n* = 3 from three independent experiments. Error bars represent SEM.

let-7 expression in the FL could recapitulate fetal or adult erythroid states, respectively, at inappropriate developmental times, effectively generating erythroid heterochronic mutants. It has been shown that *let-7* microRNAs are enriched in adult human erythroid cells compared with umbilical cord cells (Noh et al., 2009), implicating the Lin28–*let-7* axis in human developmental erythropoiesis as well. Indeed, these studies have been extended to demonstrate that the Lin28–*let-7* axis acts as a regulator of hemoglobin switching (Lee et al., 2013). Further study is necessary to delineate potential roles for *let-7* microRNAs in sequential phases of erythroid precursor differentiation.

Our RNAseq data show that CMPs from FL and adult BM differentially express transcripts characteristic of erythroid and granulocytic differentiation, in agreement with priming for production of appropriately differentiated progeny, as described previously (Pronk et al., 2007; Notta et al., 2016). Our data suggest that this priming may be regulated at least in part by Lin28 and *let-7* given the coordinate patterns of gene expression we observed between *iLIN28B* adult BM and normal FL CMPs. We identified *Hmga2* as one of the most highly up-regulated mRNAs in FLs and i*LIN28B* adult BM CMPs compared with WT adult BM CMPs, consistent with a role as a candidate effector of Lin28b/*let-7*–driven regulation of CMP output. Hmga2 has been previously implicated as a regulator of myeloid progenitor cell function (Lam et al., 2014), and consistent with our results, its ectopic expression can drive adult BM and extramedullary erythropoiesis (Ikeda et al., 2011). Interestingly, this effect parallels a study wherein insertional activation of *HMGA2* by a gene therapy lentivirus in a human β-thalassemia patient resulted in autonomous erythropoiesis and transfusional independence (Cavazzana-Calvo et al., 2010). Further supportive of an intersection with Lin28–*let-7* function, Hmga2 previously has been shown to regulate developmental timing in neural stem cells (Nishino et al., 2008).

Downloaded from http://rupress.org/jem/article-pdf/213/8/1497/1755526/jem_20151912.pdf by guest on 02 December 2025

Our data posit that the Lin28–*let-7* axis acts as a heterochronic switch within the hematopoietic system. The roles of Lin28/*let-7* as heterochronic regulators appear to be relevant in pathological contexts as well. In cancer, Lin28 acts as an oncofetal factor, whereby developmentally mistimed Lin28 expression provokes aberrant induction of fetal-like cell dedifferentiation and proliferation in certain tumors (Jiang et al., 2012; Rao et al., 2012; Nguyen et al., 2014; Urbach et al., 2014; Wang et al., 2015).

In sum, we propose that the highly conserved Lin28–*let-7*–Hmga2 signaling axis serves as a heterochronic genetic regulatory system that matches the myeloerythroid phenotype to the appropriate developmental state to meet physiological needs. We speculate that this paradigm of heterochronic regulation is applicable not only to the hematopoietic system, but also to other mammalian developmental processes.

MATERIALS AND METHODS

Mice. *iLIN28B* mice, *Lin28b*-deficient mice, and *iLet-7* mice that carry a Lin28-resistant chimeric form of *let-7g* consisting of the stem loop structure from *let-7g* fused to the loop of the LIN28-resistant miR-21 have been described previously (Zhu et al., 2011; Shinoda et al., 2013). For doxycycline-inducible expression of *LIN28B* or *let-7g*, transgenic mice were crossed to the B6.Cg-*Gt(ROSA)26Sor*$^{tm1(rtTA*M2)Jae}$/J strain (006965; The Jackson Laboratory; Hochedlinger et al., 2005). Experiments using WT adult mice and embryos used the C57BL/6J strain. All animal procedures were performed according to animal care guidelines approved by the Institutional Animal Care and Use Committee. To generate *let-7* KO mice, a mouse genomic clone containing the *let-7b* and *let-7c-2* isoforms was obtained from a genomic P1-derived artificial chromosome (PAC) library (RPCI-21 129s6/SvEvTAC). A gene replacement vector was constructed by recombineering essentially as previously described (Rodriguez et al., 2007). The final vector contained the MC1-DTA–negative selection cassette and the *loxP-PGK-EM7-NeobpA-loxP*–positive selection cassette. Targeted AB1 embryonic stem cell clones were identified by Southern blots and then used for blastocyst injections. Male chimeras were mated to 129S5 isogenic-CMV-Cre mice to remove the selection cassette. PCR sequencing was then used to confirm the presence of the 801-bp genomic deletion of *let-7b* and *let-7c-2*. The deletion breakpoints are as follows: 5′-GACCTCAAGAAG CCACAACATC-(810-bp deletion)-TACAACCTACTG CCTTCCCTGA-3′. Heterozygous mice were intercrossed to obtain homozygous mutant animals. Mutant animals used in these studies were backcrossed at least six generations into a C57BL/6 genetic background. This strain was also analyzed in separate experiments on the 129-strain background.

Flow cytometry and FACS. Cells were isolated from BM by flushing marrow cavities. Cells were isolated from FL from timed pregnancies. Cells were analyzed on a Fortessa flow cytometer or sorted on a FACS Aria (BD). The following anti–mouse fluorescence-conjugated antibodies were used: anti-B220, CD3, Ter119, Mac-1, Gr-1 conjugated to Pacific blue as a lineage cocktail, anti–c-kit–APC-Cy7, anti-CD34–FITC, and anti-CD16/32–PerCp-Cy5.5 (eBioscience and Affymetrix); anti–Sca-1–PE-Cy7; anti-Ter119–APC and anti–Gr-1–PE; anti–Mac-1–PE-Cy5 and anti-CD150–APC (BioLegend); and anti–Mac-1–AF700, anti-CD48–PE, and anti-CD71–FITC (BD). Cells were counterstained for viability with Sytox blue or propidium iodide (Thermo Fisher Scientific). Viability for cell quantification was determined using a parallel tube stained with Sytox blue.

Annexin V staining. BM mononuclear cells were isolated and immunostained with surface markers per the flow cytometry methods in the previous paragraph to delineate progenitor populations. They were then bound with annexin V APCs (eBioscience and Affymetrix) according to the manufacturer's instructions.

In vivo bromodeoxyuridine incorporation. Adult mice were injected intraperitoneally with 2 mg bromodeoxyuridine. 4 h later, BM cells were isolated and immunostained with surface markers to delineate progenitor populations, after which they were fixed and permeabilized for intracellular staining of incorporated bromodeoxyuridine with a kit from BD, according to the manufacturer's instructions.

DNA constructs. The *let-7* sponge construct was provided in pMSCV-puro and was a gift from P. Sharp (Massachusetts Institute of Technology, Boston, MA; plasmid 29766; Addgene; Kumar et al., 2008). pcDNA 3.1 WT mouse *Hmga2* was a gift from D. Bartel (Massachusetts Institute of Technology, Boston, MA; plasmid 14789; Addgene; Mayr et al., 2007). The WT mouse *Hmga2* insert was subcloned into pBabe-puro for retrovirus packaging.

Western blotting. The following antibodies were used for Western blotting: rabbit anti-LIN28B (4196; Cell Signaling Technology) and goat anti-actin (sc-1616; Santa Cruz Biotechnology, Inc.).

qPCR. RNA was isolated using TRIzol reagent (Thermo Fisher Scientific), and cDNA was synthesized using the miScript II kit (QIAGEN). Target cDNAs were detected using a SYBR green detection kit (Thermo Fisher Scientific) and gene-specific primers.

Cytology and microscopy. FL and BM mononuclear cells were stained with Wright-Giemsa and May-Grunwald stains (Sigma-Aldrich), and images were photographed.

Retroviral transduction of myeloid progenitors. Myeloid progenitors were isolated by FACS. Ecotropic retrovirus was generated by cotransfection of the appropriate retroviral vec-

Downloaded from http://rupress.org/jem/article-pdf/213/8/1497/1755526/jem_20151912.pdf by guest on 02 December 2025

tor with an ecotropic packaging plasmid. Myeloid progenitors were exposed to retroviral supernatant for 48 h in the presence of 100 ng/ml stem cell factor, 10 ng/ml IL-3, and 10 ng/ml IL-6 (all from R&D Systems), as well as 5 µg/ml polybrene (Sigma-Aldrich).

Methylcellulose culture. BM or FL mononuclear cells were resuspended and plated in methylcellulose medium according to the manufacturer's protocol (M3434; STEMCELL Technologies). In some experiments, cells were cultured in the presence of 1 µg/ml doxycycline (Sigma-Aldrich) or 2 µg/ml puromycin (Thermo Fisher Scientific).

RNAseq and data analysis. For reverse transcription and library preparation, we used a SMARTer Ultra Low RNA kit (V3) for sequencing and a Low Input Library Prep kit (Takara Bio Inc.) according to the manufacturer's protocol. The RNAseq libraries were sequenced on the HiSeq 2500 platform (Illumina) yielding 82 million raw reads per sample on average (Table S1). From the raw reads, adapter sequences were removed using a Cutadapt tool (Martin, 2011) allowing some mismatches (the specific parameters we used were −n 2 −e 0.02 −o 15). The cleaned reads were aligned to the mouse genome/transcriptome (10 mm and corresponding University of California, Santa Cruz, gene model) using TopHat2 software (Kim et al., 2013). The mean mapping rate was 81%, and this yields 67 million aligned reads per sample on average (Table S1). The RNAseq raw data and analyzed data have been deposited in NCBI's Gene Expression Omnibus (GEO) database (Edgar et al., 2002) and are accessible through GEO Series accession no. GSE72521.

To estimate expression levels for each gene, aligned reads per gene were counted using an htseq-count tool (Anders et al., 2015). Counts were then normalized and converted to counts per million and reads per kilobase per million values for further analysis using an edgeR package (Robinson et al., 2010). Differentially expressed genes between any two groups in this study were identified according to the edgeR's guidelines. Low-level expressed genes, which did not have counts per million values over 1 in at least three samples, were filtered out. Dispersions were estimated, and an exact test was performed. Most computational experiments were conducted on the Orchestra High Performance Compute Cluster at Harvard Medical School. For GSEA analysis, publicly available datasets for normal erythroblasts (GEO accession no. GSM995533), promyelocytes (GEO accession no. GSM1174469), myelocytes (GEO accession no. GSM1174470), and granulocytes (GEO accession no. GSM1174471) were used (Wong et al., 2013; Wu et al., 2014).

Complete blood count analysis. Under isoflurane anesthesia, mice were retroorbitally bled, and complete blood counts were obtained on a hematology system (Hemavet 950FS; Drew Scientific).

Immunohistochemistry. This was done at the Dana-Farber/Harvard Cancer Center Specialized Histopathology Core.

BM transplantation. BM mononuclear cells from age- and gender-matched male or female mice were directly retroorbitally injected (3×10^6 CD45.1 cells/recipient with 150 long-term HSCs [lineage$^-$, c-kit$^+$, Sca-1$^+$, CD48$^-$, and CD150$^+$]) into anesthetized, lethally irradiated (950 rads) congenic CD45.1 recipients. Recipients received trimethoprim-sulfamethoxazole in their drinking water for 4 wk after transplantation to prevent infection.

Statistics. Statistics were done with Student's *t* test unless otherwise indicated.

Online supplemental material. Table S1 shows RNAseq data comparing transcript expression between E14.5 FL and adult BM CMPs. Online supplemental material is available at http://www.jem.org/cgi/content/full/jem.20151912/DC1.

ACKNOWLEDGMENTS

We thank Joanna Han, Anna Zhao, and the Harvard Medical School Research Computing Team for RNAseq data management.

This work is supported by grants from the US National Institutes of Health: National Institute for Diabetes and Digestive and Kidney Diseases (R24-DK092760 and R24-DK49216), the National Heart, Lung, and Blood Institute (NHBLI Progenitor Cell Biology Consortium grant U01-HL100001), and the National Institute of General Medical Sciences (RO1GM107536; PN2 EY018244 and P30DK036836 to A.J. Wagers). G.Q. Daley is an associate member of the Broad Institute and an investigator of the Howard Hughes Medical Institute and the Manton Center for Orphan Disease Research. R.G. Rowe was supported by NHLBI (5T32HL007574-34). L.D. Wang was supported by a Damon Runyon-Sohn Foundation Pediatric Cancer Research fellowship (DSRG 02-12), an Alex's Lemonade Stand Foundation for Childhood Cancer Young Investigator award (31582), and a St. Baldrick's Foundation PALS Scholar award (243625).

The authors declare no competing financial interests.

Author contributions: R.G. Rowe and L.D. Wang designed the research, performed experiments, analyzed data, and wrote the manuscript. S. Coma performed experiments, analyzed data, and performed mouse husbandry. A. Rodriguez generated *let-7* KO mice. P.T. Nguyen, S. Ross, and P. Sousa performed experiments and mouse husbandry. R. Mathieu and D.S. Pearson performed experiments. A. Han analyzed RNAseq data. A.J. Wagers and G.Q. Daley supervised experiments, designed the research, and wrote the manuscript.

Submitted: 9 December 2015
Accepted: 18 May 2016

REFERENCES

Akashi, K., D. Traver, T. Miyamoto, and I.L. Weissman. 2000. A clonogenic common myeloid progenitor that gives rise to all myeloid lineages. *Nature.* 404:193–197. http://dx.doi.org/10.1038/35004599

Ambros, V., and H.R. Horvitz. 1984. Heterochronic mutants of the nematode Caenorhabditis elegans. *Science.* 226:409–416. http://dx.doi.org/10.1126/science.6494891

Anders, S., P.T. Pyl, and W. Huber. 2015. HTSeq—a Python framework to work with high-throughput sequencing data. *Bioinformatics.* 31:166–169. http://dx.doi.org/10.1093/bioinformatics/btu638

Bowie, M.B., D.G. Kent, B. Dykstra, K.D. McKnight, L. McCaffrey, P.A. Hoodless, and C.J. Eaves. 2007. Identification of a new intrinsically timed developmental checkpoint that reprograms key hematopoietic stem cell

Downloaded from http://rupress.org/jem/article-pdf/213/8/1497/1755526/jem_20151912.pdf by guest on 02 December 2025

properties. *Proc. Natl. Acad. Sci. USA.* 104:5878–5882. http://dx.doi.org/10.1073/pnas.0700460104

Cavazzana-Calvo, M., E. Payen, O. Negre, G. Wang, K. Hehir, F. Fusil, J. Down, M. Denaro, T. Brady, K. Westerman, et al. 2010. Transfusion independence and *HMGA2* activation after gene therapy of human β-thalassaemia. *Nature.* 467:318–322. http://dx.doi.org/10.1038/nature09328

Copley, M.R., S. Babovic, C. Benz, D.J. Knapp, P.A. Beer, D.G. Kent, S. Wohrer, D.Q. Treloar, C. Day, K. Rowe, et al. 2013. The Lin28b–let-7–Hmga2 axis determines the higher self-renewal potential of fetal haematopoietic stem cells. *Nat. Cell Biol.* 15:916–925. http://dx.doi.org/10.1038/ncb2783

Doulatov, S., F. Notta, K.L. Rice, L. Howell, A. Zelent, J.D. Licht, and J.E. Dick. 2009. PLZF is a regulator of homeostatic and cytokine-induced myeloid development. *Genes Dev.* 23:2076–2087. http://dx.doi.org/10.1101/gad.1788109

Edgar, R., M. Domrachev, and A.E. Lash. 2002. Gene Expression Omnibus: NCBI gene expression and hybridization array data repository. *Nucleic Acids Res.* 30:207–210. http://dx.doi.org/10.1093/nar/30.1.207

Emmrich, S., J.E. Katsman-Kuipers, K. Henke, M.E. Khatib, R. Jammal, F. Engeland, F. Dasci, C.M. Zwaan, M.L. den Boer, L. Verboon, et al. 2013. miR-9 is a tumor suppressor in pediatric AML with t(8;21). *Leukemia.* 28:1022–1032. http://dx.doi.org/10.1038/leu.2013.357

Emmrich, S., M. Rasche, J. Schöning, C. Reimer, S. Keihani, A. Maroz, Y. Xie, Z. Li, A. Schambach, D. Reinhardt, and J.H. Klusmann. 2014. *miR-99a/100~125b* tricistrons regulate hematopoietic stem and progenitor cell homeostasis by shifting the balance between TGFβ and Wnt signaling. *Genes Dev.* 28:858–874. http://dx.doi.org/10.1101/gad.233791.113

Hanna, J., K. Saha, B. Pando, J. van Zon, C.J. Lengner, M.P. Creyghton, A. van Oudenaarden, and R. Jaenisch. 2009. Direct cell reprogramming is a stochastic process amenable to acceleration. *Nature.* 462:595–601. http://dx.doi.org/10.1038/nature08592

He, S., I. Kim, M.S. Lim, and S.J. Morrison. 2011. Sox17 expression confers self-renewal potential and fetal stem cell characteristics upon adult hematopoietic progenitors. *Genes Dev.* 25:1613–1627. http://dx.doi.org/10.1101/gad.2052911

Hochedlinger, K., Y. Yamada, C. Beard, and R. Jaenisch. 2005. Ectopic expression of *Oct-4* blocks progenitor-cell differentiation and causes dysplasia in epithelial tissues. *Cell.* 121:465–477. http://dx.doi.org/10.1016/j.cell.2005.02.018

Ikeda, K., P.J. Mason, and M. Bessler. 2011. 3′UTR-truncated *Hmga2* cDNA causes MPN-like hematopoiesis by conferring a clonal growth advantage at the level of HSC in mice. *Blood.* 117:5860–5869. http://dx.doi.org/10.1182/blood-2011-02-334425

Ikuta, K., and I.L. Weissman. 1991. The junctional modifications of a T cell receptor gamma chain are determined at the level of thymic precursors. *J. Exp. Med.* 174:1279–1282. http://dx.doi.org/10.1084/jem.174.5.1279

Ikuta, K., T. Kina, I. MacNeil, N. Uchida, B. Peault, Y.H. Chien, and I.L. Weissman. 1990. A developmental switch in thymic lymphocyte maturation potential occurs at the level of hematopoietic stem cells. *Cell.* 62:863–874. http://dx.doi.org/10.1016/0092-8674(90)90262-D

Jiang, X., H. Huang, Z. Li, Y. Li, X. Wang, S. Gurbuxani, P. Chen, C. He, D. You, S. Zhang, et al. 2012. Blockade of miR-150 maturation by *MLL*-fusion/MYC/LIN-28 is required for *MLL*-associated leukemia. *Cancer Cell.* 22:524–535. http://dx.doi.org/10.1016/j.ccr.2012.08.028

Kim, D., G. Pertea, C. Trapnell, H. Pimentel, R. Kelley, and S.L. Salzberg. 2013. TopHat2: accurate alignment of transcriptomes in the presence of insertions, deletions and gene fusions. *Genome Biol.* 14:R36. http://dx.doi.org/10.1186/gb-2013-14-4-r36

Kumar, M.S., S.J. Erkeland, R.E. Pester, C.Y. Chen, M.S. Ebert, P.A. Sharp, and T. Jacks. 2008. Suppression of non-small cell lung tumor development by the *let-7* microRNA family. *Proc. Natl. Acad. Sci. USA.* 105:3903–3908. http://dx.doi.org/10.1073/pnas.0712321105

Lam, K., A. Muselman, R. Du, Y. Harada, A.G. Scholl, M. Yan, S. Matsuura, S. Weng, H. Harada, and D.E. Zhang. 2014. *Hmga2* is a direct target gene of RUNX1 and regulates expansion of myeloid progenitors in mice. *Blood.* 124:2203–2212. http://dx.doi.org/10.1182/blood-2014-02-554543

Lee, Y.T., J.F. de Vasconcellos, J. Yuan, C. Byrnes, S.J. Noh, E.R. Meier, K.S. Kim, A. Rabel, M. Kaushal, S.A. Muljo, and J.L. Miller. 2013. *LIN28B*-mediated expression of fetal hemoglobin and production of fetal-like erythrocytes from adult human erythroblasts ex vivo. *Blood.* 122:1034–1041. http://dx.doi.org/10.1182/blood-2012-12-472308

Martin, M. 2011. Cutadapt removes adapter sequences from high-throughput sequencing reads. *EMBnet.journal.* 17:10–12. http://dx.doi.org/http://dx.doi.org/10.14806/ej.17.1.200

Mayr, C., M.T. Hemann, and D.P. Bartel. 2007. Disrupting the pairing between *let-7* and *Hmga2* enhances oncogenic transformation. *Science.* 315:1576–1579. http://dx.doi.org/10.1126/science.1137999

McKinney-Freeman, S., P. Cahan, H. Li, S.A. Lacadie, H.T. Huang, M. Curran, S. Loewer, O. Naveiras, K.L. Kathrein, M. Konantz, et al. 2012. The transcriptional landscape of hematopoietic stem cell ontogeny. *Cell Stem Cell.* 11:701–714. http://dx.doi.org/10.1016/j.stem.2012.07.018

Mochizuki-Kashio, M., Y. Mishima, S. Miyagi, M. Negishi, A. Saraya, T. Konuma, J. Shinga, H. Koseki, and A. Iwama. 2011. Dependency on the polycomb gene *Ezh2* distinguishes fetal from adult hematopoietic stem cells. *Blood.* 118:6553–6561. http://dx.doi.org/10.1182/blood-2011-03-340554

Moss, E.G., R.C. Lee, and V. Ambros. 1997. The cold shock domain protein LIN-28 controls developmental timing in C. elegans and is regulated by the *lin-4* RNA. *Cell.* 88:637–646. http://dx.doi.org/10.1016/S0092-8674(00)81906-6

Nguyen, L.H., D.A. Robinton, M.T. Seligson, L. Wu, L. Li, D. Rakheja, S.A. Comerford, S. Ramezani, X. Sun, M.S. Parikh, et al. 2014. *Lin28b* is sufficient to drive liver cancer and necessary for its maintenance in murine models. *Cancer Cell.* 26:248–261. http://dx.doi.org/10.1016/j.ccr.2014.06.018

Nishino, J., I. Kim, K. Chada, and S.J. Morrison. 2008. Hmga2 promotes neural stem cell self-renewal in young but not old mice by reducing $p16^{Ink4a}$ and $p19^{Arf}$ expression. *Cell.* 135:227–239. http://dx.doi.org/10.1016/j.cell.2008.09.017

Noh, S.J., S.H. Miller, Y.T. Lee, S.H. Goh, F.M. Marincola, D.F. Stroncek, C. Reed, E. Wang, and J.L. Miller. 2009. *Let-7* microRNAs are developmentally regulated in circulating human erythroid cells. *J. Transl. Med.* 7:98. http://dx.doi.org/10.1186/1479-5876-7-98

Notta, F., S. Zandi, N. Takayama, S. Dobson, O.I. Gan, G. Wilson, K.B. Kaufmann, J. McLeod, E. Laurenti, C.F. Dunant, et al. 2016. Distinct routes of lineage development reshape the human blood hierarchy across ontogeny. *Science.* 351:aab2116. http://dx.doi.org/10.1126/science.aab2116

Oguro, H., L. Ding, and S.J. Morrison. 2013. SLAM family markers resolve functionally distinct subpopulations of hematopoietic stem cells and multipotent progenitors. *Cell Stem Cell.* 13:102–116. http://dx.doi.org/10.1016/j.stem.2013.05.014

Orkin, S.H., and L.I. Zon. 2008. Hematopoiesis: an evolving paradigm for stem cell biology. *Cell.* 132:631–644. http://dx.doi.org/10.1016/j.cell.2008.01.025

Paul, F., Y. Arkin, A. Giladi, D.A. Jaitin, E. Kenigsberg, H. Keren-Shaul, D. Winter, D. Lara-Astiaso, M. Gury, A. Weiner, et al. 2015. Transcriptional heterogeneity and lineage commitment in myeloid progenitors. *Cell.* 163:1663–1677. http://dx.doi.org/10.1016/j.cell.2015.11.013

Paulson, R.F., L. Shi, and D.C. Wu. 2011. Stress erythropoiesis: new signals and new stress progenitor cells. *Curr. Opin. Hematol.* 18:139–145. http://dx.doi.org/10.1097/MOH.0b013e32834521c8

Downloaded from http://rupress.org/jem/article-pdf/213/8/1497/1755526/jem_20151912.pdf by guest on 02 December 2025

Pelosi, A., S. Careccia, V. Lulli, P. Romania, G. Marziali, U. Testa, S. Lavorgna, F. Lo-Coco, M.C. Petti, B. Calabretta, et al. 2013. miRNA let-7c promotes granulocytic differentiation in acute myeloid leukemia. *Oncogene.* 32:3648–3654. http://dx.doi.org/10.1038/onc.2012.398

Polesskaya, A., S. Cuvellier, I. Naguibneva, A. Duquet, E.G. Moss, and A. Harel-Bellan. 2007. Lin-28 binds IGF-2 mRNA and participates in skeletal myogenesis by increasing translation efficiency. *Genes Dev.* 21:1125–1138. http://dx.doi.org/10.1101/gad.415007

Pronk, C.J., D.J. Rossi, R. Månsson, J.L. Attema, G.L. Norddahl, C.K. Chan, M. Sigvardsson, I.L. Weissman, and D. Bryder. 2007. Elucidation of the phenotypic, functional, and molecular topography of a myeloerythroid progenitor cell hierarchy. *Cell Stem Cell.* 1:428–442. http://dx.doi.org/10.1016/j.stem.2007.07.005

Rao, S., S.Y. Lee, A. Gutierrez, J. Perrigoue, R.J. Thapa, Z. Tu, J.R. Jeffers, M. Rhodes, S. Anderson, T. Oravecz, et al. 2012. Inactivation of ribosomal protein L22 promotes transformation by induction of the stemness factor, Lin28B. *Blood.* 120:3764–3773. http://dx.doi.org/10.1182/blood-2012-03-415349

Rebel, V.I., C.L. Miller, C.J. Eaves, and P.M. Lansdorp. 1996. The repopulation potential of fetal liver hematopoietic stem cells in mice exceeds that of their liver adult bone marrow counterparts. *Blood.* 87:3500–3507.

Robinson, M.D., D.J. McCarthy, and G.K. Smyth. 2010. edgeR: a Bioconductor package for differential expression analysis of digital gene expression data. *Bioinformatics.* 26:139–140. http://dx.doi.org/10.1093/bioinformatics/btp616

Rodriguez, A., E. Vigorito, S. Clare, M.V. Warren, P. Couttet, D.R. Soond, S. van Dongen, R.J. Grocock, P.P. Das, E.A. Miska, et al. 2007. Requirement of *bic/microRNA-155* for normal immune function. *Science.* 316:608–611. http://dx.doi.org/10.1126/science.1139253

Sakamoto, T., H. Ueno, K. Sonoda, T. Hisatomi, K. Shimizu, H. Ohashi, and H. Inomata. 2000. Blockade of TGF-β by in vivo gene transfer of a soluble TGF-β type II receptor in the muscle inhibits corneal opacification, edema and angiogenesis. *Gene Ther.* 7:1915–1924. http://dx.doi.org/10.1038/sj.gt.3301320

Sankaran, V.G., J. Xu, and S.H. Orkin. 2010. Advances in the understanding of haemoglobin switching. *Br. J. Haematol.* 149:181–194. http://dx.doi.org/10.1111/j.1365-2141.2010.08105.x

Shinoda, G., N. Shyh-Chang, T.Y. Soysa, H. Zhu, M.T. Seligson, S.P. Shah, N. Abo-Sido, A. Yabuuchi, J.P. Hagan, R.I. Gregory, et al. 2013. Fetal deficiency of lin28 programs life-long aberrations in growth and glucose metabolism. *Stem Cells.* 31:1563–1573. http://dx.doi.org/10.1002/stem.1423

Shyh-Chang, N., and G.Q. Daley. 2013. Lin28: primal regulator of growth and metabolism in stem cells. *Cell Stem Cell.* 12:395–406. http://dx.doi.org/10.1016/j.stem.2013.03.005

Shyh-Chang, N., H. Zhu, T. Yvanka de Soysa, G. Shinoda, M.T. Seligson, K.M. Tsanov, L. Nguyen, J.M. Asara, L.C. Cantley, and G.Q. Daley. 2013. Lin28 enhances tissue repair by reprogramming cellular metabolism. *Cell.* 155:778–792. http://dx.doi.org/10.1016/j.cell.2013.09.059

Socolovsky, M., H. Nam, M.D. Fleming, V.H. Haase, C. Brugnara, and H.F. Lodish. 2001. Ineffective erythropoiesis in Stat5a$^{-/-}$5b$^{-/-}$ mice due to decreased survival of early erythroblasts. *Blood.* 98:3261–3273. http://dx.doi.org/10.1182/blood.V98.12.3261

Takizawa, H., S. Boettcher, and M.G. Manz. 2012. Demand-adapted regulation of early hematopoiesis in infection and inflammation. *Blood.* 119:2991–3002. http://dx.doi.org/10.1182/blood-2011-12-380113

Traver, D., T. Miyamoto, J. Christensen, J. Iwasaki-Arai, K. Akashi, and I.L. Weissman. 2001. Fetal liver myelopoiesis occurs through distinct, prospectively isolatable progenitor subsets. *Blood.* 98:627–635. http://dx.doi.org/10.1182/blood.V98.3.627

Urbach, A., A. Yermalovich, J. Zhang, C.S. Spina, H. Zhu, A.R. Perez-Atayde, R. Shukrun, J. Charlton, N. Sebire, W. Mifsud, et al. 2014. Lin28 sustains early renal progenitors and induces Wilms tumor. *Genes Dev.* 28:971–982. http://dx.doi.org/10.1101/gad.237149.113

Viswanathan, S.R., and G.Q. Daley. 2010. Lin28: A microRNA regulator with a macro role. *Cell.* 140:445–449. http://dx.doi.org/10.1016/j.cell.2010.02.007

Viswanathan, S.R., G.Q. Daley, and R.I. Gregory. 2008. Selective blockade of microRNA processing by Lin28. *Science.* 320:97–100. http://dx.doi.org/10.1126/science.1154040

Viswanathan, S.R., J.T. Powers, W. Einhorn, Y. Hoshida, T.L. Ng, S. Toffanin, M. O'Sullivan, J. Lu, L.A. Phillips, V.L. Lockhart, et al. 2009. Lin28 promotes transformation and is associated with advanced human malignancies. *Nat. Genet.* 41:843–848. http://dx.doi.org/10.1038/ng.392

Wang, L.D., T.N. Rao, R.G. Rowe, P.T. Nguyen, J.L. Sullivan, D.S. Pearson, S. Doulatov, L. Wu, R.C. Lindsley, H. Zhu, et al. 2015. The role of Lin28b in myeloid and mast cell differentiation and mast cell malignancy. *Leukemia.* 29:1320–1330. http://dx.doi.org/10.1038/leu.2015.19

West, J.A., S.R. Viswanathan, A. Yabuuchi, K. Cunniff, A. Takeuchi, I.H. Park, J.E. Sero, H. Zhu, A. Perez-Atayde, A.L. Frazier, et al. 2009. A role for Lin28 in primordial germ-cell development and germ-cell malignancy. *Nature.* 460:909–913. http://dx.doi.org/10.1038/nature08210

Wong, J.J., W. Ritchie, O.A. Ebner, M. Selbach, J.W. Wong, Y. Huang, D. Gao, N. Pinello, M. Gonzalez, K. Baidya, et al. 2013. Orchestrated intron retention regulates normal granulocyte differentiation. *Cell.* 154:583–595. http://dx.doi.org/10.1016/j.cell.2013.06.052

Wong, J.J., W. Ritchie, D. Gao, K.A. Lau, M. Gonzalez, A. Choudhary, R.J. Taft, J.E. Rasko, and J. Holst. 2014. Identification of nuclear-enriched miRNAs during mouse granulopoiesis. *J. Hematol. Oncol.* 7:42. http://dx.doi.org/10.1186/1756-8722-7-42

Wu, L., L.H. Nguyen, K. Zhou, T.Y. de Soysa, L. Li, J.B. Miller, J. Tian, J. Locker, S. Zhang, G. Shinoda, et al. 2015. Precise *let-7* expression levels balance organ regeneration against tumor suppression. *eLife.* 4:e09431. http://dx.doi.org/10.7554/eLife.09431

Wu, W., C.S. Morrissey, C.A. Keller, T. Mishra, M. Pimkin, G.A. Blobel, M.J. Weiss, and R.C. Hardison. 2014. Dynamic shifts in occupancy by TAL1 are guided by GATA factors and drive large-scale reprogramming of gene expression during hematopoiesis. *Genome Res.* 24:1945–1962. http://dx.doi.org/10.1101/gr.164830.113

Xiang, J., D.C. Wu, Y. Chen, and R.F. Paulson. 2015. In vitro culture of stress erythroid progenitors identifies distinct progenitor populations and analogous human progenitors. *Blood.* 125:1803–1812. http://dx.doi.org/10.1182/blood-2014-07-591453

Xie, H., J. Xu, J.H. Hsu, M. Nguyen, Y. Fujiwara, C. Peng, and S.H. Orkin. 2014. Polycomb repressive complex 2 regulates normal hematopoietic stem cell function in a developmental-stage-specific manner. *Cell Stem Cell.* 14:68–80. http://dx.doi.org/10.1016/j.stem.2013.10.001

Yang, M., S.L. Yang, S. Herrlinger, C. Liang, M. Dzieciatkowska, K.C. Hansen, R. Desai, A. Nagy, L. Niswander, E.G. Moss, and J.F. Chen. 2015. Lin28 promotes the proliferative capacity of neural progenitor cells in brain development. *Development.* 142:1616–1627. http://dx.doi.org/10.1242/dev.120543

Yu, J., M.A. Vodyanik, K. Smuga-Otto, J. Antosiewicz-Bourget, J.L. Frane, S. Tian, J. Nie, G.A. Jonsdottir, V. Ruotti, R. Stewart, et al. 2007. Induced pluripotent stem cell lines derived from human somatic cells. *Science.* 318:1917–1920. http://dx.doi.org/10.1126/science.1151526

Yuan, J., C.K. Nguyen, X. Liu, C. Kanellopoulou, and S.A. Muljo. 2012. Lin28b reprograms adult bone marrow hematopoietic progenitors to mediate fetal-like lymphopoiesis. *Science.* 335:1195–1200. http://dx.doi.org/10.1126/science.1216557

Zhou, Y., Y.S. Li, S.R. Bandi, L. Tang, S.A. Shinton, K. Hayakawa, and R.R. Hardy. 2015. Lin28b promotes fetal B lymphopoiesis through the transcription factor Arid3a. *J. Exp. Med.* 212:569–580. http://dx.doi.org/10.1084/jem.20141510

Zhu, H., N. Shyh-Chang, A.V. Segrè, G. Shinoda, S.P. Shah, W.S. Einhorn, A. Takeuchi, J.M. Engreitz, J.P. Hagan, M.G. Kharas, et al. MAGIC Investigators. 2011. The *Lin28/let-7* axis regulates glucose metabolism. *Cell.* 147:81–94. http://dx.doi.org/10.1016/j.cell.2011.08.033

Downloaded from http://rupress.org/jem/article-pdf/213/8/1497/1755526/jem_20151912.pdf by guest on 02 December 2025